International Journal of Thermophysics, Vol. 24, No. 1, January 2003 (© 2003)

Equations of State for Technical Applications. III. Results for Polar Fluids

R. Span[1] and W. Wagner[2]

Received January 10, 2002

New functional forms have been developed for multiparameter equations of state for non- and weakly polar fluids and for polar fluids. The resulting functional forms, which were established with an optimization algorithm which considers data sets for different fluids simultaneously, are suitable as a basis for equations of state for a broad variety of fluids. The functional forms were designed to fulfil typical demands of advanced technical application with regard to the achieved accuracy. They are numerically very stable and their substance-specific coefficients can easily be fitted to restricted data sets. In this way, a fast extension of the group of fluids for which accurate empirical equations of state are available is now possible. This article deals with the results found for the polar fluids CFC-11 (trichlorofluoromethane), CFC-12 (dichlorodifluoromethane), HCFC-22 (chlorodifluoromethane), HFC-32 (difluoromethane), CFC-113 (1,1,2-trichlorotrifluoroethane), HCFC-123 (2,2-dichloro-1,1,1-trifluoroethane), HFC-125 (pentafluoroethane), HFC-134a (1,1,1,2-tetrafluoroethane), HFC-143a (1,1,1-trifluoroethane), HFC-152a (1,1-difluoroethane), carbon dioxide, and ammonia. The substance-specific parameters of the new equations of state are given as well as statistical and graphical comparisons with experimental data. General features of the new class of equations of state such as their extrapolation behavior or their numerical stability and results for non- and weakly polar fluids have been discussed in preceding articles.

KEY WORDS: ammonia; carbon dioxide; CFC-11; CFC-12; CFC-113; equation of state; fundamental equation; HCFC-22; HCFC-123; Helmholtz energy; HFC-32; HFC-125; HFC-134a; HFC-143a; HFC-152a

[1] To whom correspondence should be addressed. Lehrstuhl für Thermodynamik und Energietechnik, Universität Paderborn, D-33095 Paderborn, Germany. E-mail: Roland.Span@thet.uni-paderborn.de

[2] Lehrstuhl für Thermodynamik, Ruhr-Universität Bochum, D-44780 Bochum, Germany. E-mail: Wagner@thermo.ruhr-uni-bochum.de

0195-928X/03/0100-0111/0 © 2003 Plenum Publishing Corporation

1. INTRODUCTION

Optimized functional forms are a common feature of modern, highly accurate equations of state for well measured reference fluids. To make use of the advantages of optimized functional forms for the description of less well measured fluids, Span et al. [1] presented a new kind of optimization algorithm, which simultaneously considers data sets for different substances. The chosen functional form is not the one which yields the best results for a certain fluid, but the one which yields on average the best results for all fluids. If the considered fluids are typical representatives of a certain group of fluids, such as the group of typical polar fluids, equations of state using the simultaneously optimized functional form can be fitted to data sets for different fluids out of the same group without significant disadvantages.

As a first application, we used the simultaneous optimization algorithm to establish functional forms for equations of state which are able to satisfy advanced technical demands on accuracy for typical nonpolar and polar fluids but which are *not* intended as reference equations for well measured substances. The necessary background information on the development of the new class of equations of state, on the general aspects such as their extrapolation behavior or their numerical stability, and on the selected functional forms are given in a preceding article [2]. The required substance-specific information for the considered non- and weakly polar fluids was given in Ref. 3. This article summarizes the corresponding information for the polar fluids CFC-11 (trichlorofluoromethane), CFC-12 (dichlorodifluoromethane), HCFC-22 (chlorodifluoromethane), HFC-32 (difluoromethane), CFC-113 (1,1,2-trichlorotrifluoroethane), HCFC-123 (2,2-dichloro-1,1,1-trifluoroethane), HFC-125 (pentafluoroethane), HFC-134a (1,1,1,2-tetrafluoroethane), HFC-143a (1,1,1-trifluoroethane), HFC-152a (1,1-difluoroethane), carbon dioxide, and ammonia. In addition to these fluids, the data set for ethylene described in Ref. 3 was considered when setting up the functional form for typical polar fluids [2]. However, since the functional form established for non- and weakly polar fluids yields slightly superior results for the weakly quadrupolar fluid ethylene [3], ethylene is not discussed any further in this article.

Most of the fluids which were used to set up the functional form for polar fluids and which are discussed in this article are halogenated hydrocarbons commonly used as refrigerants. However, the primary purpose of this article is not to present new equations of state for technical applications of refrigerants for which accepted reference equations are available. The halogenated hydrocarbons were selected to show that fluids with rather different polarities can be described accurately with a single,

simultaneously optimized functional form. This could only be done for halogenated hydrocarbons since sufficiently large and accurate data sets are not available for any other group of non-associating polar fluids. For this reason, equations of state for three fully halogenated hydrocarbons with chlorine (CFCs) were also established. Even though these well-measured fluids are seldom used in technical applications, they were considered in order to extend the range of described fluids. No problems are expected for fitting equations of state using the new functional form to typical, non- or weakly-associating polar fluids not yet described; see also Ref. 2.

In Section 2, the functional form of the equations is given together with the required substance-specific parameters and coefficients. In Section 3, the performance of the new class of equations of state is discussed based on graphical and statistical comparisons with the selected experimental data for all substances.

2. THE NEW EQUATIONS OF STATE FOR POLAR FLUIDS

The new class of equations of state for technical applications to polar fluids is formulated in the reduced Helmholtz energy. As usual, the reduced Helmholtz energy is split into one part which describes the behavior of the hypothetical ideal gas (superscript o) at given values of temperature and density and a second part which describes the residual behavior (superscript r) of the real fluid. Thus, the general form of the new equations of state reads

$$\frac{a(T, \rho)}{RT} = \frac{a^{\circ}(T, \rho) + a^{\mathrm{r}}(T, \rho)}{RT} = \alpha^{\circ}(\tau, \delta) + \alpha^{\mathrm{r}}(\tau, \delta), \tag{1}$$

where a is the specific or molar Helmholtz energy, R the corresponding gas constant, T the temperature, ρ the density, $\tau = T_c/T$ the inverse reduced temperature, and $\delta = \rho/\rho_c$ the reduced density. Since the Helmholtz energy as a function of temperature and density is one of the fundamental equations known in thermodynamics, all thermodynamic properties can be calculated by combinations of α° and α^{r} and their derivatives with respect to τ and δ. For some relevant properties, the corresponding relations were given in Ref. 2; for more details, see Ref. 4.

The required relation for the ideal gas part, $\alpha^{\circ}(\tau, \delta)$, can easily be obtained from an equation for the heat capacity of the ideal gas, $c_p^{\circ}(T)$, which is known rather accurately for many technically important fluids. The development of equations for $c_p^{\circ}(T)$ and the required integration is described in detail in Ref. 4. This article focuses on the description of the

Table I. References for the Molar Masses, Critical Parameters, Acentric Factors, Dipole Moments, and Correlations Used for the Caloric Properties of the Ideal Gases of the Considered Substances

Substance	Correlation used for α^o	M ($g \cdot mol^{-1}$)	T_c (K)	p_c (MPa)	ρ_c ($kg \cdot m^{-3}$)	Reference T_c, p_c, ρ_c	ω	μ (10^{-30} C·m)
			Halogenated hydrocarbons					
CFC-11	Marx et al. [5]	137.368	471.06	4.394	565.0	[5]	0.187	1.50
CFC-12	Marx et al. [5]	120.914	385.12	4.136	565.0	[5]	0.179	1.70
HCFC-22	Wagner et al. [6]	86.469	369.28	4.989	520.0	[6]	0.221	4.74
HFC-32	Tillner-Roth and Yokozeki [7]	52.024	351.35	5.795	427.0	[8]	0.277	6.60
CFC-113	Marx et al. [5]	187.376	487.21	3.392	560.0	[5]	0.252	2.87
HCFC-123	Younglove and McLinden [9]	152.931	456.82	3.672	553.0	[10, 11]	0.283	4.52
HFC-125	Piao and Noguchi [12]	120.022	339.33	3.629	571.3	[8]	0.304	5.14
HFC-134a	Tillner-Roth and Baehr [13]	102.032	374.18	4.056	508.0	[12]	0.327	6.87
HFC-143a	Li et al. [14]	84.040	345.86	3.764	434.1	[14, 15]	0.262	7.74
HFC-152[a]	Tillner-Roth [16]	66.051	386.41	4.520	368.0	[17]	0.275	7.57
			Other polar substances					
CO_2	Span and Wagner [18]	44.010	304.1282	7.377	467.6	[18]	0.225	0[a]
Ammonia	Tillner-Roth et al. [19]	17.031	405.40	11.339	225.0	[19]	0.256	4.90

[a] Carbon dioxide is considered polar due to a qudrupole moment of $Q = 1.5 \times 10^{-39}$ C·m^2

residual part of the reduced Helmholtz energy, $\alpha^r(\tau, \delta)$. For the considered substances, references for the correlations used to describe $\alpha^o(\tau, \delta)$ are given in Table I together with the values used for the molar mass and for the critical parameters. Where necessary, critical temperatures were converted to the ITS-90 temperature scale according to the procedures described by Preston-Thomas [20] and Rusby [21]. Critical pressures were rounded to 0.001 MPa. The molar masses of the molecules were calculated based on the atomic masses published by Coplen [22] and rounded to 0.001 $g \cdot mol^{-1}$.

As discussed in Ref. 2, the simultaneous optimization algorithm resulted in the following functional form for the residual part of the reduced Helmholtz energy of typical polar fluids:

$$\begin{aligned}\alpha(\tau, \delta) &= \alpha^o(\tau, \delta) + \alpha^r(\tau, \delta) \\ &= \alpha^o(\tau, \delta) + n_1\,\delta\tau^{0.250} + n_2\,\delta\tau^{1.250} + n_3\,\delta\tau^{1.500} \\ &\quad + n_4\,\delta^3\tau^{0.250} + n_5\,\delta^7\tau^{0.875} + n_6\,\delta\tau^{2.375}\,e^{-\delta} \\ &\quad + n_7\,\delta^2\tau^{2.000}\,e^{-\delta} + n_8\,\delta^5\tau^{2.125}\,e^{-\delta} + n_9\,\delta\tau^{3.500}\,e^{-\delta^2} \\ &\quad + n_{10}\,\delta\tau^{6.50}\,e^{-\delta^2} + n_{11}\,\delta^4\tau^{4.75}\,e^{-\delta^2} + n_{12}\,\delta^2\tau^{12.5}\,e^{-\delta^3}. \end{aligned} \quad (2)$$

According to Ref. 23, the value used for the universal gas constant is

$$R_m = 8.314510\ \mathrm{J \cdot mol^{-1} \cdot K^{-1}}. \tag{3}$$

The more recent internationally agreed upon value published by Mohr and Taylor [24] became available after the work on the equations presented in this article was finished. It was not taken into account, since a shift of -0.0005% in the gas constant is negligible for the level of accuracy considered here. Where applicable, specific gas constants were calculated as

$$R = R_m / M \tag{4}$$

with the molar masses given in Table I. Values for the substance-specific coefficients n_1 to n_{12} are given in Table II.

Table III gives values for the isobaric heat capacity of the ideal gas, for the pressure, for the isobaric heat capacity and for enthalpy and entropy differences calculated from Eq. (2) in order to enable a verification of computer programs. To reproduce the caloric values exactly, the reduced ideal gas contribution, α°, has to be evaluated considering the gas constant R_{Lit} used in the reference given for α°. To do so, the reduced ideal gas contribution can be written as

$$\alpha^\circ(\tau, \delta) = \alpha^\circ_{\mathrm{Lit}}(\tau, \delta) \cdot \frac{R_{\mathrm{Lit}}}{R_{\mathrm{Eq.\ (4)}}}. \tag{5}$$

Enthalpy and entropy differences are given instead of absolute values in order to avoid confusion caused by possibly different reference states.

According to the standards in refrigeration engineering, the integration constants in the formulations for $\alpha^\circ(\tau, \delta)$ for ammonia and for the halogenated hydrocarbons were chosen in such a way that $h' = 200\ \mathrm{kJ \cdot kg^{-1}}$ and $s' = 1\ \mathrm{kJ \cdot kg^{-1} \cdot K^{-1}}$ for the saturated liquid at $T_0 = 273.15$ K. For carbon dioxide, we assumed that the enthalpy and the entropy of the ideal gas become zero at $T_0 = 298.15$ K and $p_0 = 0.101325$ MPa.

3. DISCUSSION

The goal of this project was to develop numerically stable formulations which yield reliable results when being fitted to small data sets and which satisfy the demands on the accuracy of thermodynamic property data summarized in Table IV, which is repeated from Ref. 2 for the sake of completeness. In a rather general way, it has been shown in Ref. 2 that the new equations of state satisfy the formulated requirements both with

Table II. Coefficients n_i of the Simultaneously Optimized Equations for the Helmholtz Energy of Polar Fluids, Eq. (2)

i	CFC-11 n_i	CFC-12 n_i	HCFC-22 n_i	*n*HFC-32 n_i
1	$0.10656383 \times 10^{+1}$	$0.10557228 \times 10^{+1}$	$0.96268924 \times 10^{+0}$	$0.92876414 \times 10^{+0}$
2	$-0.32495206 \times 10^{+1}$	$-0.33312001 \times 10^{+1}$	$-0.25275103 \times 10^{+1}$	$-0.24673952 \times 10^{+1}$
3	$0.87823894 \times 10^{+0}$	$0.10197244 \times 10^{+1}$	$0.31308745 \times 10^{+0}$	$0.40129043 \times 10^{+0}$
4	$0.87611569 \times 10^{-1}$	$0.84155115 \times 10^{-1}$	$0.72432837 \times 10^{-1}$	$0.55101049 \times 10^{-1}$
5	$0.29950049 \times 10^{-3}$	$0.28520742 \times 10^{-3}$	$0.21930233 \times 10^{-3}$	$0.11559754 \times 10^{-3}$
6	$0.42896949 \times 10^{+0}$	$0.39625057 \times 10^{+0}$	$0.33294864 \times 10^{+0}$	$-0.25209758 \times 10^{+0}$
7	$0.70828452 \times 10^{+0}$	$0.63995721 \times 10^{+0}$	$0.63201229 \times 10^{+0}$	$0.42091879 \times 10^{+0}$
8	$-0.17391823 \times 10^{-1}$	$-0.21423411 \times 10^{-1}$	$-0.32787841 \times 10^{-2}$	$0.37071833 \times 10^{-2}$
9	$-0.37626522 \times 10^{+0}$	$-0.36249173 \times 10^{+0}$	$-0.33680834 \times 10^{+0}$	$-0.10308607 \times 10^{+0}$
10	$0.11605284 \times 10^{-1}$	$0.19341990 \times 10^{-2}$	$-0.22749022 \times 10^{-1}$	$-0.11592089 \times 10^{+0}$
11	$-0.89550567 \times 10^{-1}$	$-0.92993833 \times 10^{-1}$	$-0.87867308 \times 10^{-1}$	$-0.44350855 \times 10^{-1}$
12	$-0.30063991 \times 10^{-1}$	$-0.24876461 \times 10^{-1}$	$-0.21108145 \times 10^{-1}$	$-0.12788805 \times 10^{-1}$

i	CFC-113 n_i	HCFC-123 n_i	HFC-125 n_i	HFC-134a n_i
1	$0.10519071 \times 10^{+1}$	$0.11169730 \times 10^{+1}$	$0.11290996 \times 10^{+1}$	$0.10663189 \times 10^{+1}$
2	$-0.28724742 \times 10^{+1}$	$-0.30745930 \times 10^{+1}$	$-0.28349269 \times 10^{+1}$	$-0.24495970 \times 10^{+1}$
3	$0.41983153 \times 10^{+0}$	$0.51063873 \times 10^{+0}$	$0.29968733 \times 10^{+0}$	$0.44645718 \times 10^{-1}$
4	$0.87107788 \times 10^{-1}$	$0.94478812 \times 10^{-1}$	$0.87282204 \times 10^{-1}$	$0.75656884 \times 10^{-1}$
5	$0.24105194 \times 10^{-3}$	$0.29532752 \times 10^{-3}$	$0.26347747 \times 10^{-3}$	$0.20652089 \times 10^{-3}$
6	$0.70738262 \times 10^{+0}$	$0.66974438 \times 10^{+0}$	$0.61056963 \times 10^{+0}$	$0.42006912 \times 10^{+0}$
7	$0.93513411 \times 10^{+0}$	$0.96438575 \times 10^{+0}$	$0.90073581 \times 10^{+0}$	$0.76739111 \times 10^{+0}$
8	$-0.96713512 \times 10^{-2}$	$-0.14865424 \times 10^{-1}$	$-0.68788457 \times 10^{-2}$	$0.17897427 \times 10^{-2}$
9	$-0.52595315 \times 10^{+0}$	$-0.49221959 \times 10^{+0}$	$-0.44211186 \times 10^{+0}$	$-0.36219746 \times 10^{+0}$
10	$0.22691984 \times 10^{-1}$	$-0.22831038 \times 10^{-1}$	$-0.35041493 \times 10^{-1}$	$-0.67809370 \times 10^{-1}$
11	$-0.14556325 \times 10^{+0}$	$-0.14074860 \times 10^{+0}$	$-0.12698630 \times 10^{+0}$	$-0.10616419 \times 10^{+0}$
12	$-0.27419950 \times 10^{-1}$	$-0.25117301 \times 10^{-1}$	$-0.25185874 \times 10^{-1}$	$-0.18185791 \times 10^{-1}$

i	HFC-143a n_i	HFC-152a n_i	Carbon dioxide n_i	Ammonia n_i
1	$0.10306886 \times 10^{+1}$	$0.95702326 \times 10^{+0}$	$0.89875108 \times 10^{+0}$	$0.73022720 \times 10^{+0}$
2	$-0.29497307 \times 10^{+1}$	$-0.23707196 \times 10^{+1}$	$-0.21281985 \times 10^{+1}$	$-0.11879116 \times 10^{+1}$
3	$0.69435230 \times 10^{+0}$	$0.18748463 \times 10^{+0}$	$-0.68190320 \times 10^{-1}$	$-0.68319136 \times 10^{+0}$
4	$0.71552102 \times 10^{-1}$	$0.63800843 \times 10^{-1}$	$0.76355306 \times 10^{-1}$	$0.40028683 \times 10^{-1}$
5	$0.19155982 \times 10^{-3}$	$0.16625977 \times 10^{-3}$	$0.22053253 \times 10^{-3}$	$0.90801215 \times 10^{-4}$
6	$0.79764936 \times 10^{-1}$	$0.82208165 \times 10^{-1}$	$0.41541823 \times 10^{+0}$	$-0.56216175 \times 10^{-1}$
7	$0.56859424 \times 10^{+0}$	$0.57243518 \times 10^{+0}$	$0.71335657 \times 10^{+0}$	$0.44935601 \times 10^{+0}$
8	$-0.90946566 \times 10^{-2}$	$0.39476701 \times 10^{-2}$	$0.30354234 \times 10^{-3}$	$0.29897121 \times 10^{-1}$
9	$-0.24199452 \times 10^{+0}$	$-0.23848654 \times 10^{+0}$	$-0.36643143 \times 10^{+0}$	$-0.18181684 \times 10^{+0}$
10	$-0.70610813 \times 10^{-1}$	$-0.80711618 \times 10^{-1}$	$-0.14407781 \times 10^{-2}$	$-0.98416660 \times 10^{-1}$
11	$-0.75041709 \times 10^{-1}$	$-0.73103558 \times 10^{-1}$	$-0.89166707 \times 10^{-1}$	$-0.55083744 \times 10^{-1}$
12	$-0.16411241 \times 10^{-1}$	$-0.15538724 \times 10^{-1}$	$-0.23699887 \times 10^{-1}$	$-0.88983219 \times 10^{-2}$

Table III. Values for Computer Program Verification

Substance	$c_p^o(T_1)^a$ (kJ·kg^{-1}·K^{-1})	$p(T_1, \rho_1)^b$ (MPa)	$c_p(T_1, \rho_1)^b$ (kJ·kg^{-1}·K^{-1})	$h_2 - h_1{}^c$ (kJ·kg^{-1})	$s_2 - s_1{}^c$ (kJ·kg^{-1}·K^{-1})
			Halogenated hydrocarbons		
CFC-11	0.6879	6.077	2.3618	129.72	0.26916
CFC-12	0.7421	11.552	1.1052	121.54	0.28621
CFC-22	0.8498	17.202	1.3137	151.95	0.37335
HFC-32	1.1421	30.358	1.8392	235.85	0.59791
CFC-113	0.8055	3.962	4.0344	131.00	0.26004
HCFC-123	0.8667	6.018	1.9509	144.33	0.29582
HFC-125	1.0745	14.620	1.3219	151.30	0.35860
HFC-134a	1.1577	14.656	1.6129	181.97	0.41386
HFC-143a	1.2785	20.152	1.6702	201.13	0.47846
HFC-152a	1.4632	21.594	2.1580	270.60	0.60934
			Other polar substances		
Carbon dioxide	1.0141	45.164	1.4994	191.33	0.60315
Ammonia	2.4759	136.271	4.1916	776.69	2.07036

[a] Calculated for $T_1 = 500$ K.
[b] Calculated for $T_1 = 500$ K and $\rho_1 = 500$ kg·m^{-3}.
[c] Calculated between $T_2 = 600$ K and $\rho_2 = 100$ kg·m^{-3} and T_1 and ρ_1.

Table IV. Demands on the Accuracy of Thermodynamic Property Data Resulting from Typical Technical Applications; See also Ref. 2

Pressure range	$\rho(p,T)$	$w(p,T)$	Uncertainty in $c_p(p,T)$	$p_s(T)$	$\rho'(T)$	$\rho''(T)$
$p \leqslant 30$ MPa[a]	±0.2%[b]	±1%–±2%[c]	±1%–±2%[c]	±0.2%[d]	±0.2%	±0.4%[d,e]
$p > 30$ MPa[f]	±0.5%	±2%	±2%	–	–	–

[a] Larger uncertainties are expected in the extended critical region.
[b] In the extended critical region $\Delta p/p$ is used instead of $\Delta\rho/\rho$.
[c] ±1% at gaseous and gas-like supercritical states, ±2% at liquid and liquid-like states.
[d] Larger relative uncertainties have to be tolerated for small vapor pressures and saturated vapor densities.
[e] Combination of the uncertainties of gas densities and vapor pressures; experimental data of this accuracy are available for only a few substances.
[f] States at pressures $p > 100$ MPa are not considered due to their limited technical relevance.

regard to their numerical stability, with regard to their reliability, and with regard to the achieved accuracy. In this section, the accuracy of the new equations of state will be discussed in more detail by substance-specific comparisons with selected data sets and with values calculated from other equations of state.

In general, the selected data sets contain all reliable experimental thermodynamic property data available for the corresponding fluid. Data at pressures above 100 MPa were not used due to their limited technical relevance. Data at pressures below 100 MPa were not used if their critically evaluated experimental uncertainty comes close to or exceeds the target uncertainty of the equation of state as summarized in Table IV and if more accurate data are available in the same range of states. Data sets were used in part if they partly overlap with more accurate data sets or if outliers in the data set could be identified. Thus, the number of selected data may be substantially smaller than the total number of data in certain data sets. In some cases, inconsistencies between data describing different properties led to the exclusion of the less accurate data. Such inconsistencies can only be detected during the development of a fundamental equation of state, which by definition yields a consistent description of different properties since all properties are calculated from derivatives of the same thermodynamic potential. In this way, sets of selected data were generated, which allow for expressive statistical comparisons between experimental data and values calculated from the new equations of state. The substance-specific discussion in the following sections focuses on these sets of selected data, which were also used to optimize the functional form of Eq. (2), see Ref. 2, and to fit the coefficients of the new equations of state.

3.1. Representation of the Critical Parameters

For reasons which were explained in Ref. 2, the new equations of state were not constrained to the selected critical parameters given in Table I. Table V summarizes the critical parameters resulting from of the new equations of state, Eq. (2), in combination with the parameters given in Tables I and II, and the differences between these values and the values selected from the literature.

For most of the considered substances, critical temperatures resulting from Eq. (2) agree with the selected values within several tenths of a kelvin. Compared to the results found for non- and weakly polar fluids [3], deviations between true and calculated critical temperatures are larger on average. However, for an equation of state which is designed mainly for technical applications, this agreement is still sufficient. The enlarged deviations can be explained by the fact that the data situation in the extended

Table V. Critical Parameters Resulting from an Evaluation of the New Equations of State and Deviations from the Selected Critical Parameters Given in Table I

Substance	$T_{c,\,Eq.\,(2)}$ [a] (K)	$p_{c,\,Eq.\,(2)}$ (MPa)	$\rho_{c,\,Eq.\,(2)}$ [a] ($kg \cdot m^{-3}$)	ΔT_c (K)	Δp_c (%)	$\Delta \rho_c$ (%)	Δp_c^* [b] (%)
Halogenated Hydrocarbons							
CFC-11	469.524	4.305	507.75	−1.536	−2.037	−10.13	0.039
CFC-12	385.404	4.151	544.72	0.284	0.353	−3.59	−0.141
HCFC-22	369.429	5.003	501.73	0.149	0.277	−3.51	0.000
HFC-32	351.656	5.834	425.89	0.306	0.667	−0.26	0.014
CFC-113	487.834	3.423	536.93	0.624	0.923	−4.12	0.041
HCFC-123	457.420	3.698	519.24	0.600	0.694	−6.10	−0.235
HFC-125	339.377	3.632	536.51	0.047	0.074	−6.09	−0.025
HFC-134a	374.697	4.094	491.98	0.517	0.930	−3.15	−0.103
HFC-143a	346.704	3.826	420.37	0.844	1.643	−3.16	−0.130
HFC-152a	386.898	4.556	356.53	0.488	0.787	−3.12	0.133
Other polar substances							
Carbon dioxide	304.307	7.400	446.62	0.179	0.314	−4.45	−0.086
Ammonia	405.535	11.382	237.42	0.135	0.380	5.52	0.131

[a] $T_{c,\,Eq.\,(2)}$ and $\rho_{c,\,Eq.\,(2)}$ result from an iteration of the critical point of Eq. (2). To calculate the reduced density δ and the inversely reduced temperature τ, the values given in Table I have to be used.

[b] $\Delta p_c^* / \% = 100[\, p_{c,\,Eq.} - p_c - (T_{c,\,Eq.} - T_c)(\partial p / \partial T)_\rho |_{T_c, \rho_c}\,] / p_c$.

critical region is rather poor for most of the halogenated hydrocarbons. For carbon dioxide and ammonia, for which accurate data are available for thermal properties in the extended critical region, the calculated critical temperatures agree with the true values within less than ± 0.2 K. A significantly worse result was found for CFC-11, where no data are available for the thermal properties in the extended critical region. However, reasonable values for the critical temperature did not have to be enforced for the considered polar substances; see Ref. 3 for comparison.

Critical pressures resulting from Eq. (2) deviate from the true critical pressures by more than the $\pm 0.2\%$ claimed for the uncertainty of pressures calculated in the critical region. However, the deviations mainly result from shifted critical temperatures in combination with the steep slope of the vapor pressure curve close to the critical point. In general, pseudo-critical pressures p_c^* which are corrected for this effect agree with the selected literature values well within $\pm 0.2\%$, indicating that pressures in the immediate vicinity of the critical point can be calculated within the claimed uncertainty.

In most cases, critical densities calculated from Eq. (2) are too small by 3 to 6%. Considering the large density gradients in the immediate vicinity of the critical point, the simplicity of the new equations of state, and their main focus, this result is also regarded as reasonable. For ammonia, the calculated critical density is too large by 5.5%. Results for this fluid will be discussed in more detail in Section 3.13.

3.2. Results for CFC-11 (Trichlorofluoromethane)

The data set which is available for the refrigerant CFC-11 covers the temperature range from the triple-point temperature at $T_t \approx 162.7$ K ($T_t/T_c \approx 0.345$) to $T_{max} \approx 595$ K ($T_{max}/T_c \approx 1.26$). However, reliable $p\rho T$ data are available only at temperatures from 254 K ($T/T_c \approx 0.54$) to 477 K ($T/T_c \approx 1.01$) and at pressures up to 31 MPa. No reliable experimental data are available for thermal properties in the extended critical region, and the data situation at gaseous states is also poor. At higher temperatures and pressures, data are available only for speeds of sound and isobaric heat capacities. The selected data set was restricted to pressures $p \leqslant 100$ MPa. With regard to vapor-liquid equilibrium states, reliable experimental results are available for the vapor pressure, for the saturated liquid density, and for the isobaric heat capacity and the speed of sound of the saturated liquid. Reliable data are lacking for the saturated vapor density. Reviews on the available data set were published by Marx et al. [5] and Jacobsen et al. [25].

Table VI summarizes the data sets selected for this project. The given number of data corresponds to the number of selected data points; the total number of points in the corresponding data set can be substantially larger. Statistical information on the accuracy of the equation is given as percentage average absolute deviations,

$$\%\,AAD = \frac{100}{N} \cdot \sum_{i=1}^{N} \left| \frac{y_{calc} - y_{exp}}{y_{exp}} \right|, \tag{6}$$

for six regions, namely for the gas phase and the liquid phase at subcritical temperatures, for the extended critical region defined as $0.98 \leqslant T/T_c \leqslant 1.1$ and $0.7 \leqslant \rho/\rho_c \leqslant 1.4$, and for the supercritical fluid subdivided into a low-density range (LD, $\rho/\rho_c \leqslant 0.6$), a medium-density range (MD, $0.6 < \rho/\rho_c < 1.5$), and a high-density range (HD, $\rho/\rho_c \geqslant 1.5$). Data in the liquid and supercritical high-density range often correspond to states at $p \geqslant 30$ MPa. Thus, larger density deviations in these ranges may still be acceptable; see Table IV. For $p\rho T$ data in the extended

Table VI. Summary of the Data Sets Selected for CFC-11 and Average Absolute Deviations Between Values Calculated from the New Equation of State and the Selected Data

Authors	No. of data	Temperature and pressure range T (K)	p (MPa)	Average absolute deviations (AAD), % Gas	Liq.	Crit. reg.	Supercritical fluid LD[a]	MD[a]	HD[a]
***pρT* data**[b]									
Benning and McHarness [26]	34	303–477	0.1–2.1	0.264	–	–	0.176	–	–
Kremenevskaja and Rivkin [27]	66	383–473	0.5–4.0	0.159	–	–	0.318	–	–
Rivkin and Kremenevskaja [28]	147	273–473	0.8–20.0	–	0.062	–	–	–	0.086
Kolebev and Shaemardanov [29]	40	278–315	0.2–6.8	–	0.042	–	–	–	–
Blanke [30]	84	269–355	2.1–29.9	–	0.020	–	–	–	–
Blanke [31]	42	254–269	0.7–9.9	–	0.014	–	–	–	–
Blanke [32]	77	331–454	3.2–31.3	–	0.014	–	–	–	–
Blanke and Weiß [33]	76	254–454	0.7–31.3	–	0.044	–	–	–	–
Speeds of sound									
Kolomov et al. [34]	104	243–471	0.0–2.2	0.341	–	–	0.492	–	–
Meyer [35]	21	197–293	0.1	–	0.994	–	–	–	–
Chavez et al. [36]	68	163–452	Sat. liq.	–	1.331	–	–	–	–
Lainez et al. [37]	57	353–413	9.4–100	–	0.316	–	–	–	–
Isobaric/saturated liquid heat capacities									
Osborne et al. [38]	13	171–288	Sat. liq.	–	0.681	–	–	–	–
Grishkov and Sirota [39]	92	326–595	2.5–19.6	–	0.415	1.535	–	1.095	0.962
Wirbser et al. [40]	69	288–503	0.6–30.0	–	0.349	–	0.877	–	0.700
Second virial coefficients									
Hirschfelder et al. [41]	9	239–450	–	1.869	–	–	–	–	–

Authors	No of data	Temp. range T (K)	Average absolute deviations (AAD), % $T/T_c < 0.6$	$0.6 \leqslant T/T_c \leqslant 0.98$	$T/T_c > 0.98$
Vapor pressures[d]					
Riedel [42]	12	224–328	0.702	0.112	–
Osborne et al. [38]	7	237–293	0.093	0.058	–
Kremenevskaja and Rivkin [43]	57	343–463	–	0.202	0.215
Fernandez-Fassnacht and Del Rio [44]	30	223–291	0.177	0.026	–
Saturated liquid densities					
Benning and McHarness [45]	14	273–464	0.064	0.108	0.436
Kriebel and Löffler [46]	5	253–293	0.052	0.070	–
Okada et al. [47]	12	283–363	–	0.080	–
Okada et al. [48]	14	263–453	0.125	0.088	–

[a] LD: $\rho/\rho_c \leqslant 0.6$; MD: $0.6 < \rho/\rho_c < 1.5$; HD: $\rho/\rho_c \geqslant 1.5$.
[b] In the extended critical region, pressure deviations are given instead of density deviations.
[c] At temperatures $T/T_c < 0.6$, average absolute deviations in hPa are given.

critical region, deviations in pressure are given instead of deviations in density; see also Table IV. Results for vapor pressures and saturated liquid and vapor densities are reported separately for three temperature ranges. At very low reduced temperatures ($T/T_c < 0.6$), relative deviations between measured and calculated vapor pressures increase due to the very small absolute values of the vapor pressure. Thus, average absolute deviations in hPa[3] are reported for vapor pressures in this temperature range. For the saturated vapor density, enlarged relative deviations are expected if data are at all available at low reduced temperatures. At temperatures close to the critical temperature ($T/T_c > 0.98$), relative deviations of the saturation densities increase due to large absolute values of the gradients and of the saturated liquid density, ρ', and the saturated vapor density, ρ'', respectively. In this range, the representation of vapor pressures is a more reasonable measure for the quality of technical equations of state.

As can be seen from Table VI, the new equation of state generally represents the selected data within the demanded uncertainties. Significantly larger deviations are observed only for speeds of sound in the saturated liquid, where the limit of $|\Delta w|/w \leqslant 2\%$ is exceeded for temperatures below ≈ 180 K with maximum deviations of $\Delta w'/w' \approx -3.5\%$. Similar problems were also found for some non- and weakly polar fluids [3]. It is very difficult to obtain an accurate description of speeds of sound in the liquid phase at temperatures close to the triple-point temperature with technical equations of state; existing technical equations of state mostly yield results which are far worse than those found for the new equation for CFC-11 [2, 4]. In most technical applications, fluids are used at temperatures well above the triple-point temperature. Thus, the observed deviations are still considered as satisfactory.

Based on the results reported in Table VI, it seems as if the new equation yields a poor description of thermal properties at gaseous states and of vapor pressures at high temperatures. However, in both cases the large average absolute deviations are caused by inconsistencies of the available experimental data. Figure 1 shows deviations between selected experimental results for the vapor pressure of CFC-11 and values calculated from the new equation of state, Eq. (2). Values calculated from the reference equations of state by Marx et al. [5] and Jacobsen et al. [25] are plotted for comparison. Accurate data for the vapor pressure of CFC-11 are available only at moderate temperatures. At higher temperatures, the data by Kremenevskaya and Rivkin [43] show experimental scatter which clearly exceeds $\pm 0.2\%$, and which is responsible for the larger average absolute deviations reported in Table VI, even though the data are represented

[3] 10^2 Pa; 1 hPa corresponds to 1mbar.

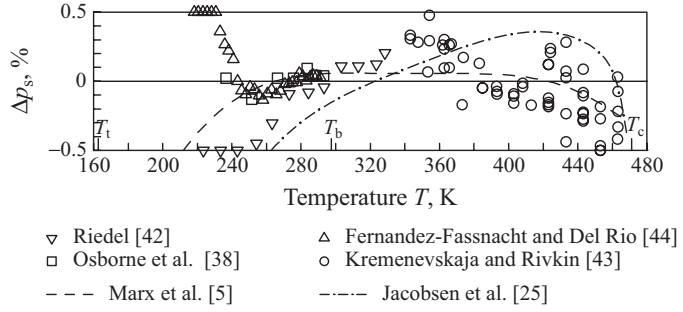

Fig. 1. Percentage deviations Δp_s, $\% = 100\,(p_{s,\,exp} - p_{s,\,calc})/p_{s,\,exp}$ between selected experimental results for the vapor pressure of CFC-11 and values calculated from the new equation of state, Eq. (2). Values calculated from the reference equations by Marx et al. [5] and Jacobsen et al. [25] are plotted for comparison.

basically within their scatter. Enlarged relative deviations at temperatures below 240 K can be attributed to the very low vapor pressures at these states.

Figure 2 shows deviations between selected experimental data for the density of CFC-11 and values calculated from Eq. (2). Values calculated from the reference equations of state by Marx et al. [5] and Jacobsen et al. [25] are again plotted for comparison. In the liquid phase, accurate experimental data are represented well within the demanded uncertainty of $|\Delta\rho|/\rho \leqslant 0.2\%$. However, in the gas phase the inconsistencies between the most accurate available data sets exceed $\pm 0.2\%$. These inconsistencies result in the larger average absolute deviations reported in Table VI.

3.3. Results for CFC-12 (Dichlorodifluoromethane)

The data set for the refrigerant CFC-12 covers the temperature range from the triple-point temperature at $T_t \approx 116.1$ K($T_t/T_c \approx 0.301$) to $T_{max} \approx 475$ K ($T_{max}/T_c \approx 1.23$); the data set used was restricted to pressures of $p \leqslant 100$ MPa. With regard to thermal properties, the data situation is satisfactory with shortcomings only in the extended critical region. Highly accurate $pρT$ data became available at gaseous and liquid states with the data set published by Händel et al. [49]. Data for caloric properties are available only up to pressures of $p = 6.4$ MPa. At vapor-liquid equilibrium states, reliable data are again available for the vapor pressure, for the saturated liquid density, and for the isobaric heat capacity and the speed of sound of the saturated liquid. Accurate experimental results were published for the saturated vapor density only at three temperatures. More detailed

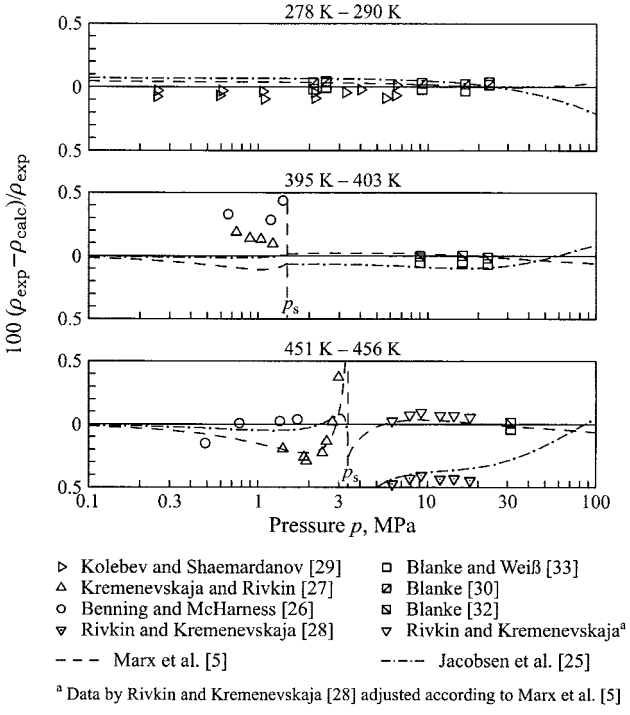

Fig. 2. Percentage deviations between selected experimental results for the density of CFC-11 and values calculated from the new equation of state, Eq. (2). Values calculated from the reference equations by Marx et al. [5] and Jacobsen et al. [25] are plotted for comparison.

reviews on the available data were published by Marx et al. [5] and Penoncello et al. [50]. Table VII summarizes the data sets selected for this project and gives percentage average absolute deviations between the selected experimental data and values calculated from the new equation of state, Eq. (2). The saturated vapor densities measured by Händel et al. [49] were not used to fit Eq. (2), but were used to show that equations of this type are able to predict saturated vapor densities within the demanded uncertainty of $|\Delta\rho''|/\rho'' \leqslant 0.4\%$ based on experimental data in the gas phase and for the vapor pressure.

In general, Eq. (2) represents the available data sets well within the demanded uncertainties. However, among the studied polar substances, CFC-12 is the one with the smallest reduced triple-point temperature. Typical problems which have been reported for low temperature liquid

states become more pronounced for R-12. For homogeneous states, accurate $p\rho T$ data at temperatures as low as 150 K ($T/T_c \approx 0.389$) are represented well within the demanded uncertainty of $|\Delta\rho|/\rho \leqslant 0.2\%$. However, for saturated liquid states at very low temperatures, larger deviations are observed for ρ', c'_p, and w', as shown in Fig. 3. While the reference equation by Marx et al. [5] represents the experimental data for all three properties very well, Eq. (2) yields values which are too large especially for the caloric properties. These systematic deviations are responsible for the slightly larger weighted variance reported for CFC-12

Table VII. Summary of the Data Sets Selected for CFC-12 and Average Absolute Deviations Between Values Calculated from the New Equation of State and the Selected Data

Authors	No. of data	Temperature and pressure range T (K)	p (MPa)	Average absolute deviations (AAD), % Gas	Liq.	Crit. reg.	Supercritical fluid LD[a]	MD[a]	HD[a]
***pρT* data**[b]									
Michels et al. [51]	182	323–423	0.7–8.2	0.086	–	0.120	0.035	0.162	–
Perel'shtein [52]	42	341–471	0.8–4.8	0.050	–	–	0.027	–	–
Watanabe et al. [53]	86	283–403	0.1–4.4	0.093	–	–	0.062	–	–
Kumagai and Iwasaki [54]	16	253–313	9.7–85.3	–	0.067	–	–	–	–
Oguchi et al. [55]	25	293–353	0.9–29.5	–	0.055	–	–	–	–
Iglesias-Silva [56]	56	230–475	0.7–68.3	–	0.036	–	–	–	0.027
Blanke et al. [57]	33	264–423	2.1–30.2	–	0.059	–	–	–	0.065
Blanke [58]	35	244–267	0.8–9.8	–	0.032	–	–	–	–
Blanke [31]	94	326–462	2.7–30.0	–	0.055	–	–	–	0.020
Händel et al. [49]	85	150–330	0.1–8.0	0.105	0.069	–	–	–	–
Isochoric heat capacities									
Hwang [59]	7	395–458	1.4–1.7	–	–	–	0.770	–	–
Speeds of sound									
Woodburn et al. [60]	22	297–362	0.4–0.7	0.443	–	–	–	–	–
Sheludyakov et al. [61]	88	233–363	0.0–2.7	0.310	–	–	–	–	–
Meyer [35]	14	198–235	0.1	–	1.679	–	–	–	–
Poole and Aziz [62]	20	117–198	Sat. Liq.	–	1.185	–	–	–	–
Winters and Merte [63]	1	300	Sat. Liq.	–	1.594	–	–	–	–
Tam and Leung [64]	1	295	0.1	0.858	–	–	–	–	–
Isobaric/saturated liquid heat capacities									
Masi [65]	11	243–363	0.0–0.2	0.254	–	–	–	–	–
McHarness et al. [66]	17	169–253	Sat. Liq.	–	0.881	–	–	–	–
Ernst [67]	26	293–363	0.1–0.8	0.393	–	–	–	–	–
Gruzdev and Shumskaya [68]	54	305–459	0.6–2.0	1.265	–	–	0.215	–	–
Enthalpy differences									
Castro-Gomez [69]	11	246–415	1.6–6.4	–	0.939	–	–	–	–
Second virial coefficients									
Michels et al. [51]	15	323–423	–	0.657	–	–	–	–	–
Schramm [70]	13	233–296	–	1.765	–	–	–	–	–

Table VII. *(Continued)*

Authors	No of data	Temp. range T (K)	Average absolute deviations (AAD), % $T/T_c < 0.6$	$0.6 \leqslant T/T_c \leqslant 0.98$	$T/T_c > 0.98$
Vapor pressures[c]					
Michels et al. [51]	9	298–384	–	0.082	0.213
Oguchi et al. [71]	20	303–383	–	0.090	0.011
Blanke and Weiß [72]	12	205–244	0.404	0.039	–
Händel et al. [49]	23	260–330	–	0.051	–
Saturated liquid densities					
Okada et al. [47]	3	343–363	–	0.155	–
Händel et al. [49]	23	120–340	0.132	0.058	–
Saturated vapor densities					
Händel et al. [49]	3[d]	260–330	–	0.251	–

[a] LD: $\rho/\rho_c \leqslant 0.6$; MD: $0.6 < \rho/\rho_c < 1.5$; HD: $\rho/\rho_c \geqslant 1.5$.
[b] In the extended critical region, pressure deviations are given instead of density deviations.
[c] At temperatures $T/T_c < 0.6$, average absolute deviations in hPa are given.
[d] Data used only for comparison.

in Ref. 2. Results from the reference equation by Penoncello et al. [50] are shown in Fig. 3 in the range where the equation is valid ($T \geqslant 175$ K). When extrapolated to liquid states close to the triple point, it yields negative values for the isobaric heat capacity and correspondingly unreasonable results for other caloric properties.

3.4. Results for HCFC-22 (Chlorodifluoromethane)

The data set which was used for the refrigerant HCFC-22 covers a temperature range from almost the triple-point temperature at $T_t \approx 115.7$ K ($T_t/T_c \approx 0.313$) to $T_{max} \approx 524$ K ($T_{max}/T_c \approx 1.42$). The data set used was restricted to pressures $p \leqslant 100$ MPa. Both with regard to thermal and caloric properties, the data situation is clearly better than for the other "old" refrigerants. State-of-the-art data are available for the $p\rho T$ relation, for the isobaric heat capacity, for the speed of sound at liquid and gaseous states, and for thermal properties on the phase boundary including some accurate results for the saturated vapor density. A detailed review on the available data set was published by Wagner et al. [6] together with a reference equation of state. Kamei et al. [73] presented a reference equation for HCFC-22 as well, but they did not discuss data sets in much detail. Table VIII summarizes the data sets selected for this project and gives percentage average absolute deviations between the selected experimental data

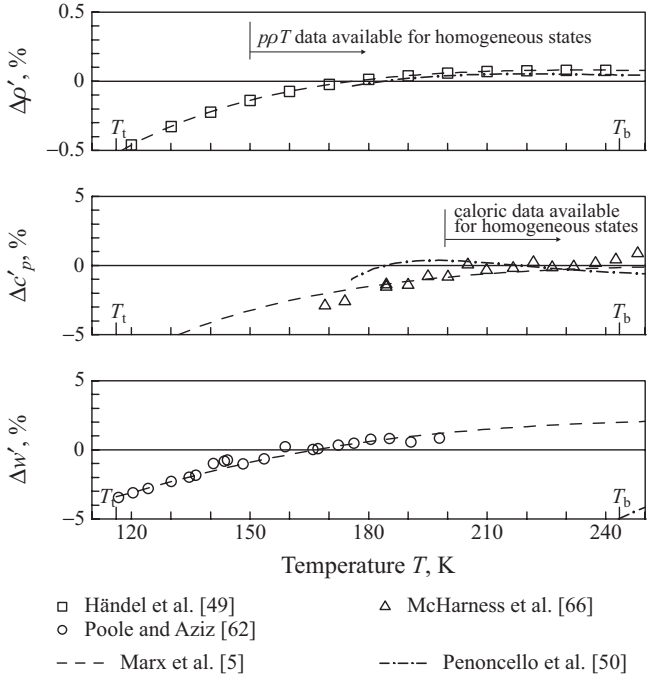

Fig. 3. Percentage deviations Δy, $\% = 100\ (y_{exp} - y_{calc})/y_{exp}$ with $y = \rho'$, c'_p, and w' between selected experimental results for low temperature saturated liquid states of CFC-12 and values calculated from the new equation of state, Eq. (2). Values calculated from the reference equations by Marx et al. [5] and Penoncello et al. [50] are plotted for comparison.

and values calculated from the new equation of state, Eq. (2). Again, the saturated vapor densities measured by Händel et al. [49] were not used to fit Eq. (2).

The new equation of state generally satisfies the demands on accuracy summarized in Table IV. To give an example of this capability, Fig. 4 shows the representation of selected speed of sound data on three isotherms at gaseous and liquid states. The representation of the saturated vapor densities by Händel et al. [49] shows that such data can be predicted even within $|\Delta\rho''|/\rho'' \approx 0.1\%$ if the equation is based on accurate data for the vapor pressure and for properties in the gas phase. At temperatures below 130 K, calculated values for the saturated liquid density deviate from accurate experimental results by up to $\Delta\rho'/\rho' \approx -0.3\%$ and calculated values for the liquid heat capacity at saturation deviate by up to

$\Delta c_\sigma / c_\sigma \approx -3\%$. These slightly larger deviations result from the fact that the reduced triple-point temperature of HCFC-22, T_t/T_c, is very low; see Section 3.3 for comparison. At temperatures above 450 K, slightly larger deviations are observed for $p\rho T$ data at densities around the critical density corresponding to pressures of about 20 MPa. This effect may be attributed to the fact that accurate data at far supercritical states were available for

Table VIII. Summary of the Data Sets Selected for HCFC-22 and Average Absolute Deviations Between Values Calculated from the New Equation of State and the Selected Data

Authors	No. of data	Temperature and pressure range T (K)	p (MPa)	Average absolute deviations (AAD), % Gas	Liq.	Crit. reg.	Supercritical fluid LD[a]	MD[a]	HD[a]
***pρT* data**[b]									
Michels [74]	158	292–398	0.7–9.2	0.032	–	0.102	0.031	0.351	–
Kletskii [75]	54	294–465	0.8–5.8	0.098	–	0.050	0.023	–	–
Kumagai and Iwasaki [54]	18	253–313	9.7–84.8	–	0.128	–	–	–	–
Oguchi et al. [76]	45	292–363	1.2–11.3	–	0.063	–	–	–	–
Kohlen et al. [77]	90	252–523	2.1–60.6	–	0.044	–	–	–	0.061
Kohlen [78]	133	338–488	0.1–16.8	0.038	–	–	0.017	0.120	–
Blanke et al. [57]	54	269–325	2.2–29.8	–	0.041	–	–	–	–
Blanke and Weiß [58]	79	246–289	1.2–10.1	–	0.016	–	–	–	–
Blanke and Weiß [79]	45	120–249	1.1–4.6	–	0.091	–	–	–	–
Fukuizumi and Uematsu [80]	85	310–400	1.5–10.0	–	0.037	0.119	–	0.161	0.037
Händel et al. [49]	55	150–330	0.1–8.1	0.049	0.054	–	–	–	–
Niesen et al. [81]	18	304–372	1.2–15.4	–	0.021	–	–	–	0.058
Isochoric heat capacities									
Hwang [59]	37	323–443	1.5–3.5	0.471	–	–	1.116	–	–
Speeds of sound									
Novikov and Lagutina [82]	73	293–373	0.2 –5.0	0.189	–	–	0.274	–	–
Meyer [35]	9	198–226	0.1	–	0.984	–	–	–	–
Niepmann [83]	106	200–300	2.5–60.1	–	0.660	–	–	–	–
Lemming [84]	104	270–350	0.1–0.5	0.008	–	–	–	–	–
Isobaric/saturated liquid heat capacities									
Neilson and White [85]	9	122–194	Sat. liq.	–	1.216	–	–	–	–
Ernst and Büsser [86]	37	293–353	0.1–1.4	0.550	–	–	–	–	–
Bier et al. [87]	15	333–353	0.2–2.9	0.257	–	–	–	–	–
Gruzdev and Shumskaya [68]	55	302–452	0.9–2.0	0.871	–	–	0.713	–	–
Ernst and Wirbser [88]	100	280–500	2.0–30.0	0.629	0.501	0.185	0.795	0.716	0.584
Joule-Thomson coefficients									
Bier et al. [89]	38	293–473	0.3–1.5	0.510	–	–	0.957	–	–
Günther and Stephan [90,91]	25	318–408	0.3–7.0	0.388	–	0.661	0.302	0.606	–
Second virial coefficients									
Schramm and Weber [92]	8	243–296	–	2.348	–	–	–	–	–
Händel et al. [49]	3	270–330	–	1.002	–	–	–	–	–

Table VIII. *(Continued)*

Authors	No of data	Temp. range T (K)	Average absolute deviations (AAD), % $T/T_c < 0.6$	$0.6 \leqslant T/T_c \leqslant 0.98$	$T/T_c > 0.98$
Vapor pressures[c]					
Kriebel [93]	9	213–293	0.302	0.047	–
Kletskii [75]	20	195–369	0.071	0.060	0.038
Oguchi et al. [76]	17	253–363	–	0.023	0.075
Takaishi et al. [94]	13	305–364	–	0.023	0.040
Blanke and Weiss [72]	10	186–240	0.206	0.032	–
Fukuizumi and Uematsu [95]	5	310–350	–	0.030	–
Händel et al. [49]	30	230–340	–	0.033	–
Saturated liquid densities					
Kletskii [75]	5	359–366	–	0.175	0.256
Oguchi et al. [76]	6	292–345	–	0.079	–
Händel et al. [49]	25	120–340	0.121	0.066	–
Saturated vapor densities					
Händel et al. [49]	4[d]	250–330	–	0.066	–

[a] LD: $\rho/\rho_c \leqslant 0.6$; MD: $0.6 < \rho/\rho_c < 1.5$; HD: $\rho/\rho_c \geqslant 1.5$.
[b] In the extended critical region, pressure deviations are given instead of density deviations.
[c] At temperatures $T/T_c < 0.6$, average absolute deviations in hPa are given.
[d] Data used only for comparison.

only a few of the polar fluids considered when setting up the simultaneously optimized functional form of Eq. (2). For more details, see Section 3.12 and Ref. 2.

3.5. Results for HFC-32 (Difluoromethane)

The data set for the refrigerant HFC-32 covers the temperature range from the triple-point temperature at $T_t \approx 136.2$ K ($T_t/T_c \approx 0.388$) to $T_{max} \approx 420$ K ($T_{max}/T_c \approx 1.20$) at pressures up to $p_{max} \approx 72$ MPa. An intensive investigation of the thermodynamic properties of the "alternative," non-ozone depleting refrigerant HFC-32 began in the early 1990s. The data set which is available today is smaller than the data sets for refrigerants such as CFC-12 or HCFC-22, but most of the data were measured with modern experimental equipment, and thus the data set is more consistent than average data sets for the "old" refrigerants—the number of "selected" data is larger than that for HCFC-22. Similar situations were also found for the "new" refrigerants discussed in Sections 3.7 to 3.11. Data for thermal properties are available both in homogeneous and at vapor-liquid equilibrium states, with restrictions for the supercritical fluid at medium densities

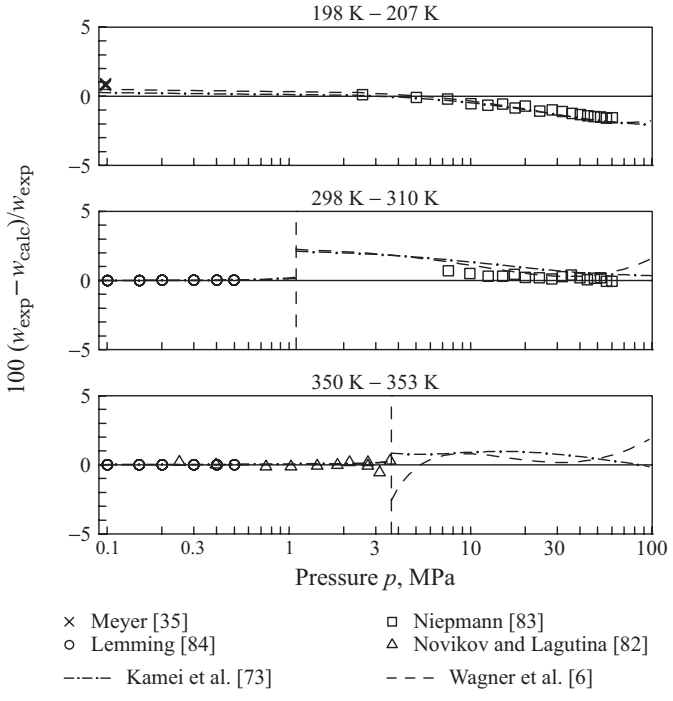

Fig. 4. Percentage deviations between selected experimental results for the speed of sound in HCFC-22 and values calculated from the new equation of state, Eq. (2). Values calculated from the reference equations by Wagner et al. [6] and Kamei et al. [73] are plotted for comparison.

where there are only a few points available from two different authors. For the saturated vapor density, reasonable data are available from about the normal boiling temperature to the critical temperature. Accurate experimental results for caloric properties are mostly available for just liquid states. A detailed review of the available data sets was published by Tillner-Roth and Yokozeki [7]. Table IX summarizes the data sets selected for this project and gives percentage average absolute deviations between the selected experimental data and values calculated from the new equation of state, Eq. (2).

In general, the new equation of state represents the available data within the demanded uncertainties. Slightly larger deviations, up to $|\Delta p|/p \approx 0.3\%$, are observed only for states in the extended critical region close to T_{max}, where data are scarce. As an example of the representation of

Table IX. Summary of the Data Sets Selected for HFC-32 and Average Absolute Deviations Between Values Calculated from the New Equation of State and the Selected Data

Authors	No. of data	Temperature and pressure range T (K)	p (MPa)	Average absolute deviations (AAD), % Gas	Liq.	Crit. reg.	Supercritical fluid LD[a]	MD[a]	HD[a]
***pρT* data**[b]									
Holste et al. [96]	94	150–375	1.5–71.7	–	0.100	–	–	–	0.132
Quian et al. [97]	56	300–370	0.2–6.5	0.080	–	0.073	0.045	–	–
Bouchot and Richon [98]	26	253–333	0.3–9.5	0.127	0.086	–	–	–	–
Defibaugh et al. [99]	343	243–373	0.2–9.8	0.098	0.079	0.102	0.092	–	–
Sato et al. [100]	58	322–420	3.3–9.8	0.288	0.120	0.056	0.093	0.540	0.068
Magee [101]	137	140–396	3.6–35.1	–	0.076	–	–	–	0.044
Zhang et al. [102]	81	290–370	0.1–6.5	0.067	–	0.090	0.070	–	–
DeVries [103]	474	263–383	0.0–20.6	0.050	–	0.092	0.039	0.234	0.156
Isochoric heat capacities									
Lüddecke and Magee [104]	73	153–341	5.4–32.6	–	0.755	–	–	–	–
Speeds of sound									
Grebenkov et al. [105]	30	287–341	1.5–10.4	–	0.661	–	–	–	–
Hozumi et al. [106]	67	273–343	0.0–0.3	0.012	–	–	–	–	–
Isobaric/saturated liquid heat capacities									
Lüddecke and Magee [104]	101	141–342	Sat. liq.	–	0.679	–	–	–	–
Yomo et al. [107]	26	276–315	2.1–3.0	–	1.707	–	–	–	–
Second virial coefficients									
Sato et al. [100]	9	340–420	–	4.133	–	–	–	–	–
Zhang et al. [102]	9	290–370	–	1.204	–	–	–	–	–

Authors	No of data	Temp. range T (K)	Average absolute deviations (AAD), % $T/T_c < 0.6$	$0.6 \leqslant T/T_c \leqslant 0.98$	$T/T_c > 0.98$
Vapor pressures[c]					
Malbrunot et al. [108]	12	191–253	0.636	0.237	–
Kanungo et al. [109]	4	149–175	0.221	–	–
Holcomb et al. [110]	21	316–349	–	0.101	0.048
Quian et al. [97]	9	280–350	–	0.044	0.052
Weber and Goodwin [111]	27	208–237	0.521	0.054	–
Defibaugh et al. [99]	18	268–348	–	0.029	0.031
Sato et al. [100]	21	320–351	–	0.060	0.017
Weber and Silva [112]	16	236–266	–	0.085	–
Nagel and Bier [113]	27	204–351	1.238	0.066	0.023
Magee [101]	7	270–330	–	0.079	–
DeVries [103]	112	298–351	–	0.045	0.040
Saturated liquid densities					
Holcomb et al. [110]	25	295–349	–	0.063	0.246
Bouchot and Richon [98]	5	253–333	–	0.072	–
Defibaugh et al. [99]	21	243–338	–	0.064	–
Magee [101]	13	139–305	0.154	0.060	–
Saturated vapor densities					
Holcomb et al. [110]	20	321–349	–	0.213	0.226
Defibaugh et al. [99]	28	219–343	–	0.191	–

[a] LD: $\rho/\rho_c \leqslant 0.6$; MD: $0.6 < \rho/\rho_c < 1.5$; HD: $\rho/\rho_c \geqslant 1.5$.
[b] In the extended critical region, pressure deviations are given instead of density deviations.
[c] At temperatures $T/T_c < 0.6$, average absolute deviations in hPa are given.

caloric properties at liquid states, Fig. 5 shows deviations between experimental results for the isochoric heat capacity and values calculated from Eq. (2).

3.6. Results for CFC-113 (1,1,2-Trichlorotrifluoroethane)

For the refrigerant CFC-113, only a very limited data set is available which covers the temperature range from the triple-point temperature at $T_t \approx 236.9$ K ($T_t/T_c \approx 0.486$) to $T_{max} \approx 538$ K ($T_{max}/T_c \approx 1.10$) at pressures up to $p_{max} \approx 30$ MPa. Thermal properties of the homogeneous region and saturated liquid are described with sufficient accuracy, but at gaseous and supercritical states the data situation is unsatisfactory. The representation of caloric properties is based mainly on experimental results for the isobaric heat capacity. No data for the saturated vapor density and for caloric properties on the vapor-liquid phase boundary could be incorporated in the

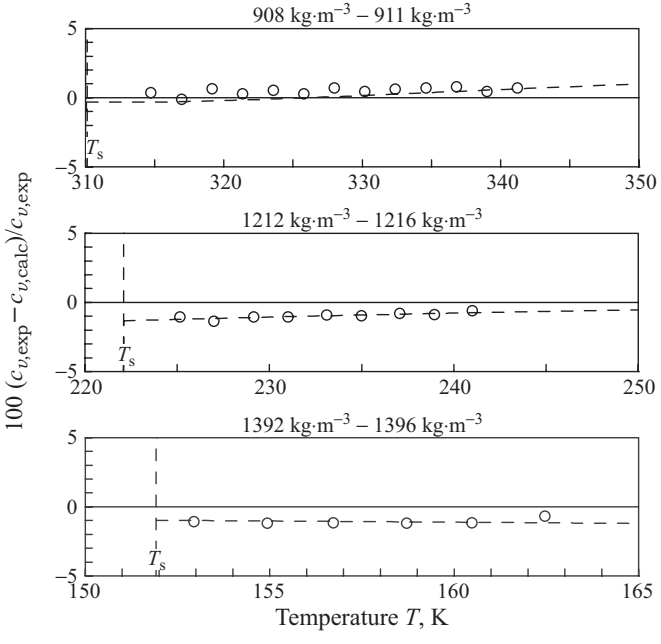

Fig. 5. Percentage deviations between selected experimental results for the isochoric heat capacity of HFC-32 and values calculated from the new equation of state, Eq. (2). Values calculated from the reference equation by Tillner-Roth and Yokozeki [7] are plotted for comparison.

Table X. Summary of the Data Sets Selected for CFC-113 and Average Absolute Deviations Between Values Calculated from the New Equation of State and the Selected Data

Authors	No. of data	Temperature and pressure range T (K)	p (MPa)	Average absolute deviations (AAD), % Gas	Liq.	Crit. reg.	Supercritical fluid LD[a]	MD[a]	HD[a]
***pρT* data**[b]									
Riedel [114]	17	294–360	0.0–0.2	0.097	–	–	–	–	–
Geller [115]	157	253–508	0.5–24.3	–	0.034	–	–	–	0.066
Mastroianni et al. [116]	21	405–538	0.8–6.2	0.077	–	0.183	0.117	0.168	–
Blanke [31]	88	266–354	2.1–29.9	–	0.009	–	–	–	–
Blanke [32]	71	331–453	3.1–30.4	–	0.031	–	–	–	–
Blanke and Weiß [33]	60	266–453	2.1–30.4	–	0.021	–	–	–	–
Speeds of sound									
Meyer [35]	16	239–293	0.1	–	0.653	–	–	–	–
Isobaric heat capacities									
Ernst and Büsser [85]	10	293–353	0.0–0.2	0.110	–	–	–	–	–
Vesloguzov [117]	34	361–452	0.1–1.1	0.414	–	–	–	–	–
Ponomareva [118]	61	260–410	1.0–10.0	–	0.336	–	–	–	–
Wirbser et al. [40]	79	303–503	0.6–30.0	–	0.429	–	0.587	–	0.344

Authors	No of data	Temp. range T (K)	Average absolute deviations (AAD), % $T/T_c < 0.6$	$0.6 \leqslant T/T_c \leqslant 0.98$	$T/T_c > 0.98$
Vapor pressures[d]					
Riedel [114]	13	259–352	0.122	0.038	–
Varushenko and Bulgatova [119]	6	298–317	–	0.036	–
Mastroianni et al. [116]	11	263–485	0.200	0.078	0.005
Saturated liquid densities					
Varushenko and Bulgatova [119]	3	293–303	–	0.072	–
Okada et al. [48]	23	243–463	0.062	0.073	–

[a] LD: $\rho/\rho_c \leqslant 0.6$; MD: $0.6 < \rho/\rho_c < 1.5$; HD: $\rho/\rho_c \geqslant 1.5$.
[b] In the extended critical region, pressure deviations are given instead of density deviations.
[c] At temperatures $T/T_c < 0.6$, average absolute deviations in hPa are given.

set of selected experimental data. A detailed review of the available data set was given by Marx et al. [5]. Table X summarizes the data sets selected for this project and gives percentage average absolute deviations between the selected experimental data and values calculated from the new equation of state, Eq. (2).

The new equation of state for CFC-113 describes the available data for thermal and caloric properties well within the demanded uncertainties. However, experimental information on supercritical states in the range of

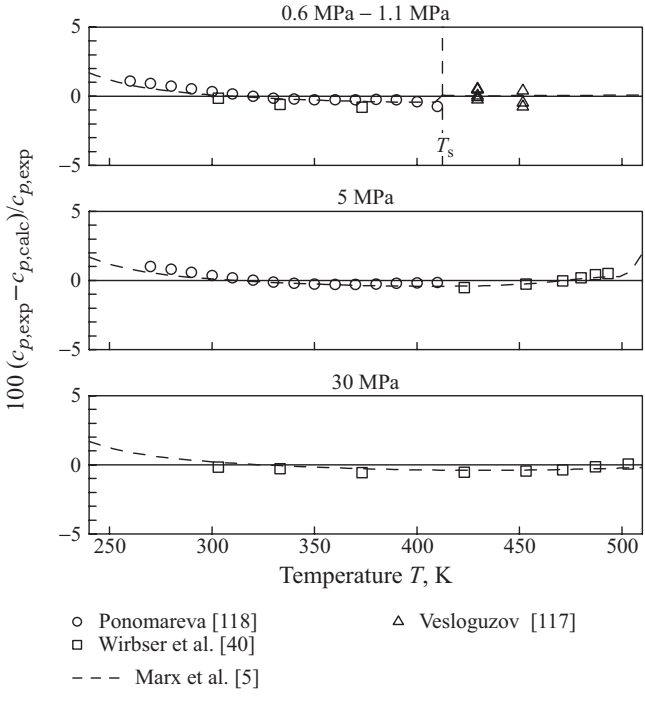

Fig. 6. Percentage deviations between selected experimental results for the isobaric heat capacity of CFC-113 and values calculated from the new equation of state, Eq. (2). Values calculated from the reference equations by Marx et al. [5] are plotted for comparison.

medium densities is scarce. In this range, an enlarged uncertainty of $|\Delta\rho|/\rho \leqslant 0.4\%$ has to be assumed for values calculated from Eq. (2). As an example of the representation of caloric properties, Fig. 6 shows deviations between selected experimental data for the isobaric heat capacity at gaseous, liquid, and supercritical states and values calculated from Eq. (2). Since the data set for CFC-113 is the most limited among the data sets considered in this article, ideal curves calculated with the new equation for CFC-113 were shown in Ref. 2 to discuss the numerical stability and the extrapolation behavior of the new functional form for polar fluids.

3.7. Results for HCFC-123 (2,2-Dichloro-1,1,1-trifluoroethane)

At pressures up to $p_{\max} \approx 76$ MPa, the data set which is available for the refrigerant HCFC-123 covers the temperature range from the triple-point temperature at $T_t \approx 166.0$ K ($T_t/T_c \approx 0.363$) to $T_{\max} \approx 523$ K

($T_{max}/T_c \approx 1.14$). However, at pressures of $p > 39$ MPa, experimental results are available for just the speed of sound in liquid states. For gaseous and liquid states, sufficient $p\rho T$ data are available, but there are significant inconsistencies between the different data sets. At supercritical temperatures, the data situation becomes questionable even for the development of a technical equation of state. Accurate experimental data are available for the vapor pressure and the saturated liquid density. The data sets available for the saturated vapor density allow for an accuracy of $|\Delta\rho''|/\rho'' \leqslant 0.5\%$ up to $T=423$ K ($T/T_c \approx 0.93$). At higher temperatures, the available data scatter by more than $\pm 1\%$. Reliable caloric data are essentially available only for liquid states. A review of the available experimental data was published by Younglove and McLinden [9]. Table XI summarizes the data sets selected for this project and gives percentage average absolute deviations between the selected experimental data and values calculated from the new equation of state, Eq. (2).

In general, the simultaneously optimized equation of state represents the available data within the demanded uncertainties. Based on the results summarized in Table XI, it seems as if the representation of the gas-phase $p\rho T$ data by Piao et al. [124] is extremely poor. However, these data are located very close to the critical region; except for two points, the corresponding deviations in pressure remain within $|\Delta p|/p \leqslant 0.2\%$. Significantly larger deviations are observed only for the heat capacity of the saturated liquid, c_σ, at temperatures close to the triple-point temperature. The limit of $|\Delta c_\sigma|/c_\sigma \leqslant 2\%$ is exceeded for $T < \approx 185$ K, with deviations up to $\Delta c_\sigma/c_\sigma \approx -4\%$ at T_t. Figure 7 shows the representation of selected $p\rho T$ data on two typical subcritical isotherms.

3.8. Results for HFC-125 (Pentafluoroethane)

The data set which was used for refrigerant HFC-125 covers the temperature range from the triple-point temperature at $T_t \approx 172.5$ K ($T_t/T_c \approx 0.508$) to $T_{max} \approx 400$ K ($T_{max}/T_c \approx 1.18$) at pressures up to $p_{max} \approx 68$ MPa. Although all of the data result from recent experimental investigations, significant inconsistencies are observed among the available data sets especially for thermal properties. In the extended critical region, the data situation is scarce. For vapor-liquid equilibrium states, accurate data are available for the vapor pressure, the saturated liquid density, and the saturated liquid heat capacity. At temperatures above 293 K ($T/T_c > 0.86$), data are available for the speed of sound in the saturated liquid and vapor phase as well. Reliable experimental results for the saturated vapor density are lacking, except for some data in the extended critical region. For homogeneous states, accurate caloric data are available

for both the gas and liquid phase. More detailed reviews of the available data set have been published by Piao and Noguchi [12] and by Sunaga et al. [140]. Table XII summarizes the data sets selected for this project and gives percentage average absolute deviations between the selected experimental data and values calculated from the new equation of state, Eq. (2).

In general, the new equation of state represents the selected data well within the demanded uncertainties. Figure 8 shows the representation of

Table XI. Summary of the Data Sets Selected for HCFC-123 and Average Absolute Deviations Between Values Calculated from the New Equation of State and the Selected Data

Authors	No. of data	Temperature and pressure range T (K)	p (MPa)	Average absolute deviations (AAD), % Gas	Liq.	Crit. reg.	Supercritical fluid LD[a]	MD[a]	HD[a]
***pρT* data**[b]									
Matsuo [120]	42	293–353	0.1–38.8	–	0.080	–	–	–	–
Maezawa et al. [121]	8	280–340	0.5–2.0	–	0.063	–	–	–	–
Weber [122]	73	358–453	0.2–2.1	0.070	–	–	–	–	–
Morrison and Ward [123]	78	280–364	0.3–3.8	–	0.028	–	–	–	–
Piao et al. [124]	110	311–523	0.5–12.0	1.349	0.049	0.106	0.167	0.307	0.064
Oguchi et al. [125]	35	352–493	0.8–16.4	0.293	0.080	0.072	0.063	–	0.108
Magee [126]	90	193–343	0.5–34.5	–	0.061	–	–	–	–
Magee and Howley [127]	105	176–380	0.4–34.5	–	0.064	–	–	–	–
Isochoric heat capacities									
Magee [126]	79	196–341	1.4–32.3	–	1.125	–	–	–	–
Speeds of sound									
Goodwin and Moldover [128]	42	260–335	0.0–0.1	0.010	–	–	–	–	–
Takagi [129]	195	283–373	0.1–75.7	–	0.715	–	–	–	–
Isobaric/saturated liquid heat capacities									
Nakagawa et al. [130]	144	276–440	0.5–3.2	–	0.998	–	–	–	–
Magee [126]	90	167–304	Sat. liq.	–	1.081	–	–	–	–
Second virial coefficients									
Goodwin and Moldover [128]	12	260–453	–	1.422	–	–	–	–	–

Authors	No of data	Temp. range T (K)	Average absolute deviations (AAD), % $T/T_c < 0.6$	$0.6 \leqslant T/T_c \leqslant 0.98$	$T/T_c > 0.98$
Vapor pressures[c]					
Yamashita et al. [131]	37	278–453	–	0.066	0.046
Weber [122]	44	338–453	–	0.122	0.047
Morrison and Ward [123]	6	280–364	–	0.162	–
Piao et al. [124]	64	308–457	–	0.085	0.041
Buschmeier et al. [132]	17	343–423	–	0.021	–
Weber [133]	13	278–308	–	0.077	–
Magee [126]	6	160–260	0.201	–	–

Table XI. *(Continued)*

Authors	No of data	Temp. range T (K)	Average absolute deviations (AAD), % $T/T_c < 0.6$	$0.6 \leqslant T/T_c \leqslant 0.98$	$T/T_c > 0.98$
Saturated liquid densities					
Oguchi and Takaishi [134]	10	254–343	0.066	0.069	–
Schmidt [135]	6	274–373	–	0.081	–
Fukushima [136]	2	425–441	–	0.202	–
Fukushima et al. [11]	9	445–457	–	0.109	0.917
Tanikawa et al. [10]	16	401–457	–	0.067	0.509
Weber and Levelt Sengers [137]	12	333–456	–	0.121	0.423
Fukushima [138]	11	281–352	–	0.111	–
Morrison and Ward [123]	11	280–364	–	0.039	–
Yokoyama and Takahashi [139]	27	251–423	0.116	0.049	–
Buschmeier et al. [132]	27	293–423	–	0.070	–
Magee [126]	8	174–328	0.093	0.026	–
Saturated vapor densities					
Weber and Levelt Sengers [137]	3	448–453	–	–	0.734
Buschmeier et al. [132]	26	299–423	–	0.339	–

[a] LD: $\rho/\rho_c \leqslant 0.6$; MD: $0.6 < \rho/\rho_c < 1.5$; HD: $\rho/\rho_c \geqslant 1.5$.
[b] In the extended critical region, pressure deviations are given instead of density deviations.
[c] At temperatures $T/T_c < 0.6$, average absolute deviations in hPa are given.

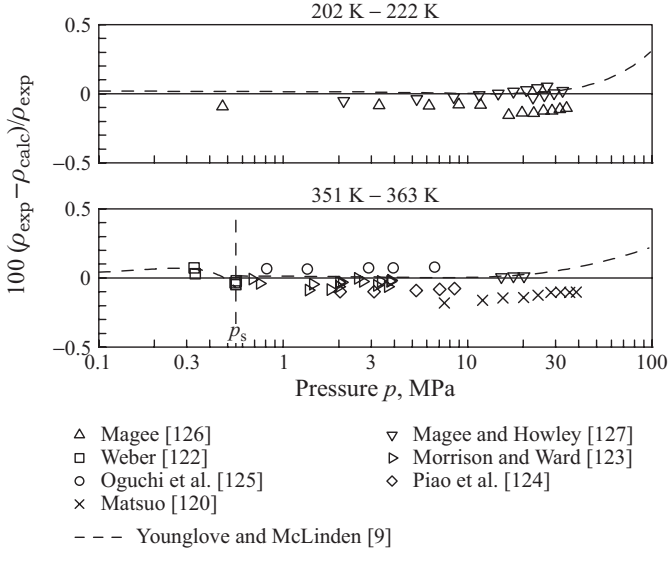

Fig. 7. Percentage deviations between selected experimental results for the density of HCFC-123 and values calculated from the new equation of state, Eq. (2). Values calculated from the reference equation by Younglove and McLinden [9] are plotted for comparison.

speed of sound data for homogeneous and saturated states. Values calculated from the reference equations of state by Piao and Noguchi [12] and by Sunaga et al. [140] are plotted for comparison. The experimental data for gaseous, liquid and supercritical states are represented far within the limits claimed in Table IV. Speeds of sound in the saturated liquid and

Table XII. Summary of the Data Sets Selected for HFC-125 and Average Absolute Deviations Between Values Calculated from the New Equation of State and the Selected Data

Authors	No. of data	Temperature and pressure range T (K)	p (MPa)	Average absolute deviations (AAD), % Gas	Liq.	Crit. reg.	Supercritical fluid LD[a]	MD[a]	HD[a]
***pρT* data**[b]									
Defibaugh and Morrison [141]	123	275–369	1.6–6.3	–	0.067	0.064	0.091	0.106	0.022
Boyes and Weber [142]	91	273–363	0.3–4.6	0.058	–	–	0.048	–	–
Ye et al. [143]	9	390	0.2–3.4	–	–	–	0.025	–	–
Magee [101]	79	178–398	3.6–35.4	–	0.037	–	–	–	0.040
Zhang et al. [102]	84	290–390	0.1–3.6	0.066	–	–	0.029	–	–
Duarte-Garza et al. [144]	145	180–350	1.2–68.0	–	0.079	–	–	–	0.106
DeVries [103]	287	263–343	0.0–19.8	0.053	–	0.135	0.034	–	0.126
Isochoric heat capacities									
Lüddecke and Magee [104]	99	200–342	3.9–33.0	–	0.543	–	–	–	0.471
Speeds of sound									
Grebenkov et al. [105]	30	288–333	1.1–16.4	–	0.236	–	–	–	–
Kraft and Leipertz [145]	17	293–338	Saturated	0.675	1.618	5.211	–	–	–
Hozumi et al. [146]	72	273–343	0.0–0.2	0.034	–	–	0.041	–	–
Gillis [147]	149	240–400	0.0–1.0	0.019	–	–	0.013	–	–
Saturated liquid heat capacities									
Lüddecke and Magee [104]	93	176–278	Sat. liq.	–	0.272	–	–	–	–
Second virial coefficients									
Bignell and Dunlop [148]	2	290–300	–	0.383	–	–	–	–	–
Zhang et al. [102]	11	290–390	–	0.947	–	–	–	–	–
Gillis [147]	9	240–400	–	0.681	–	–	–	–	–

Authors	No of data	Temp. range T (K)	Average absolute deviations (AAD), % $T/T_c < 0.6$	$0.6 \leqslant T/T_c \leqslant 0.98$	$T/T_c > 0.98$
Vapor pressures[c]					
Monluc et al. [149]	19	313–339	–	0.041	0.046
Wilson et al. [150]	18	195–327	3.572	0.127	–
Sagawa [151]	17	313–339	–	0.036	0.092
Sagawa et al. [152]	26	308–339	–	0.021	0.036
Weber and Silva [112]	66	219–335	–	0.025	0.034
Boyes and Weber [142]	29	273–335	–	0.021	0.022
Ye et al. [143]	12	290–339	–	0.071	0.049
Magee [101]	13	215–335	–	0.111	0.176
DeVries [103]	80	303–339	–	0.006	0.028

Table XII. *(Continued)*

Authors	No of data	Temp. range T (K)	Average absolute deviations (AAD), % $T/T_c < 0.6$	$0.6 \leqslant T/T_c \leqslant 0.98$	$T/T_c > 0.98$
Saturated liquid densities					
Defibaugh and Morrison [141]	7	276–332	–	0.131	–
Higashi [153]	6	325–339	–	0.228	0.642
Kuwabara et al. [154]	10	333–339	–	–	1.207
Magee [101]	7	173–308	0.035	0.072	–
Saturated vapor densities					
Higashi [153]	2	338–339	–	–	2.274
Kuwabara et al. [154]	8	336–339	–	–	1.935

[a] LD: $\rho/\rho_c \leqslant 0.6$; MD: $0.6 < \rho/\rho_c < 1.5$; HD: $\rho/\rho_c \geqslant 1.5$.
[b] In the extended critical region, pressure deviations are given instead of density deviations.
[c] At temperatures $T/T_c < 0.6$, average absolute deviations in hPa are given.

vapor are represented within $|\Delta w|/w \leqslant 2\%$ up to reduced temperatures of $T/T_c \approx 0.96$ and $T/T_c \approx 0.99$, respectively. Bearing in mind that speeds of sound in the critical region cannot be accurately described by rather simple technical equations of state for fundamental reasons (see, e.g., Ref. 4), these results are considered to be excellent.

In a comparison with all available data, the new technical equation of state, Eq. (2), yields results which are on average more accurate than those of the reference equation by Piao and Noguchi [12], while the reference equation by Sunaga et al. [140] is slightly superior to Eq. (2).

3.9. Results for HFC-134a (1,1,1,2-Tetrafluoroethane)

Among the halogenated methanes and ethanes, the data set which is available for the thermodynamic properties of the refrigerant HFC-134a is the most extensive. Accurate experimental data are available for thermal and caloric properties from the triple-point temperature at $T_t \approx 169.9$ K ($T_t/T_c \approx 0.454$) up to $T_{max} \approx 523$ K ($T_{max}/T_c \approx 1.40$) and at pressures to $p_{max} \approx 75$ MPa. Significant inconsistencies, even between recent data sets, are again observed, but for HFC-134a the data situation is good enough to identify sets of reliable reference data. On the vapor-liquid phase boundary, accurate experimental data are available for the vapor pressure, for the saturated liquid density and for the heat capacity of the saturated liquid. Data for the saturated vapor density are available, but most of the data scatter by more than $\pm 0.5\%$. A detailed review of the available data set

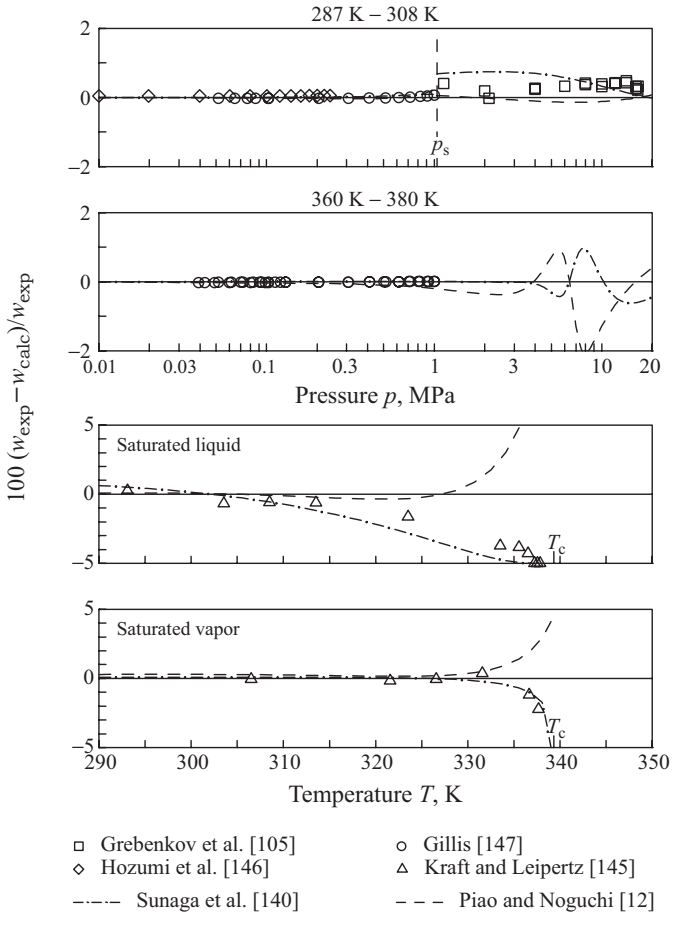

Fig. 8. Percentage deviations between selected experimental results for the speed of sound in HFC-125 and values calculated from the new equation of state, Eq. (2). Values calculated from the reference equations by Piao and Noguchi [12] and Sunaga et al. [140] are plotted for comparison.

has been published by Tillner-Roth and Baehr [13]. Table XIII summarizes the data sets selected for this project and gives percentage average absolute deviations between the selected experimental data and values calculated from the new equation of state, Eq. (2).

In general, the new equation of state represents the selected data well within the demanded accuracy. Slightly larger deviations are observed only

for $p\rho T$ data at supercritical states in the range of medium densities. This fact is illustrated in Fig. 9, which shows selected $p\rho T$ data on three isotherms covering gaseous, liquid and supercritical states. As an example of the representation of caloric properties at liquid states, Fig. 10 shows deviations between the saturated liquid heat capacities measured by Magee [159] and values calculated from Eq. (2).

Table XIII. Summary of the Data Sets Selected for HFC-134a and Average Absolute Deviations Between Values Calculated from the New Equation of State and the Selected Data

Authors	No. of data	Temperature and pressure range T (K)	p (MPa)	Average absolute deviations (AAD), % Gas	Liq.	Crit. reg.	Supercritical fluid LD[a]	MD[a]	HD[a]
***pρT* data**[b]									
Weber [155]	69	321–423	0.2–5.3	0.117	–	–	0.129	–	–
Piao et al. [156]	81	314–423	1.1–11.8	0.065	0.063	0.076	0.067	0.120	0.133
Morrison and Ward [123]	93	279–338	0.7–5.8	–	0.042	–	–	–	–
Tang et al. [157]	147	365–450	3.2–15.9	0.393	0.114	0.055	0.047	0.147	0.049
Hou et al. [158]	288	180–340	0.8–70.9	–	0.041	–	–	–	–
Magee [159]	150	187–343	2.6–34.9	–	0.087	–	–	–	–
Quian et al. [160]	21	320–340	0.1–1.9	0.050	–	–	–	–	–
Tillner-Roth and Baehr [161]	410	293–453	0.1–16.4	0.034	–	0.070	0.024	0.158	0.060
Dressner and Bier [162]	121	333–423	0.3–57.8	0.039	–	0.061	0.037	0.156	0.055
Klomfar et al. [163]	89	204–310	1.1–56.3	–	0.063	–	–	–	–
Tillner-Roth and Baehr [164]	428	243–413	0.7–15.8	0.179	0.026	0.073	0.101	0.143	0.049
Isochoric heat capacities									
Magee [159]	150	187–343	2.6–34.6	–	0.368	–	–	–	–
Speeds of sound									
Goodwin and Moldover [165]	94	233–340	0.0–0.6	0.015	–	–	–	–	–
Takagi [166]	80	290–370	2.0–75.0	–	0.358	–	–	–	–
Tang et al. [157]	122[c]	367–450	3.5–18.9	3.058	1.955	4.023	2.171	1.026	0.912
Guedes and Zollweg [167]	206	179–380	0.1–69.5	–	0.402	3.143	–	1.829	0.504
Beckermann [168]	244	260–420	0.0–0.5	0.020	–	–	0.033	–	–
Isobaric/saturated liquid heat capacities									
Saitoh et al. [169]	29	276–356	1.0–3.0	–	0.302	–	–	–	–
Nakagawa et al. [170]	34	273–356	0.5–3.0	–	0.309	–	–	–	–
Ernst et al. [171][d]	172	253–523	0.0–30.0	0.642	0.308	0.860	0.445	0.539	0.309
Magee [159]	160	172–290	Sat. liq.	–	0.270	–	–	–	–
Enthalpy differences									
Blanke et al. [173]	18	180–240	Evaporation	0.215	–	–	–	–	
Joule-Thomson coefficients									
Wirbser [172]	102	333–423	0.3–20.0	0.978	1.475	6.224	0.849	2.583	2.612
Second virial coefficients									
Weber [155]	11	323–423	–	0.578	–	–	–	–	–
Goodwin and Moldover [165]	15	235–440	–	0.965	–	–	–	–	–
Beckermann [168]	9	260–420	–	0.606	–	–	–	–	–
Ernst et al. [171]	7	333–423	–	0.681	–	–	–	–	–
Quian et al. [160]	3	320–340	–	0.841	–	–	–	–	–
Tillner-Roth and Baehr [161]	19	293–453	–	0.531	–	–	–	–	–

Table XIII. *(Continued)*

Authors	No of data	Temp. range T (K)	Average absolute deviations (AAD), % $T/T_c < 0.6$	$0.6 \leqslant T/T_c \leqslant 0.98$	$T/T_c > 0.98$
Vapor pressures[e]					
Baehr and Tillner-Roth [174]	37	303–374	–	0.047	0.080
Magee and Howley [175]	6	180–220	0.249	–	–
Goodwin et al. [176]	57	214–313	0.375	0.063	–
Saturated liquid densities					
Morrison and Ward [123]	26	268–368	–	0.124	0.470
Yokoyama and Takahashi [139]	21	252–367	–	0.050	0.384
Saturated vapor densities					
Weber [155]	5	320–366	–	0.157	–

[a] LD: $\rho/\rho_c \leqslant 0.6$; MD: $0.6 < \rho/\rho_c < 1.5$; HD: $\rho/\rho_c \geqslant 1.5$.
[b] In the extended critical region, pressure deviations are given instead of density deviations.
[c] Calculated data, used with reduced weighting factors.
[d] See also Ref. [172].
[e] At temperatures $T/T_c < 0.6$, average absolute deviations in hPa are given.

3.10. Results for HFC-143a (1,1,1-Trifluoroethane)

The data set for the refrigerant HFC-143a covers the temperature range from the triple-point temperature at $T_t \approx 161.3$K ($T_t/T_c \approx 0.466$) to $T_{max} \approx 433$ K ($T_{max}/T_c \approx 1.25$) at pressures up to $p_{max} \approx 35$ MPa. Within these limits, a sufficient number of accurate $p\rho T$ data is available for all homogeneous states and accurate experimental results for the vapor pressure and the saturated liquid density are available at least for temperatures above about 200 K and 245 K, respectively. No data could be selected for the saturated vapor density. Significant inconsistencies can again be observed between different sets of recent $p\rho T$ data, but based on the demands on the accuracy of technical equations of state, these inconsistencies can be tolerated. State-of-the-art experimental results for caloric properties are published for gaseous and liquid states. Recently, reviews of the available data sets were published by Li et al. [14] and Lemmon and Jacobsen [177]. Table XIV summarizes the data sets selected for this project and gives percentage average absolute deviations between the selected experimental data and values calculated from the new equation of state, Eq. (2).

The new equation of state for HFC-143a represents the selected data within the demanded uncertainties without reservation. As an example of the representation of thermal properties in the extended critical region, Fig. 11 shows percentage deviations between experimental results for the $p\rho T$ relation of HFC-143a and pressures calculated from Eq. (2).

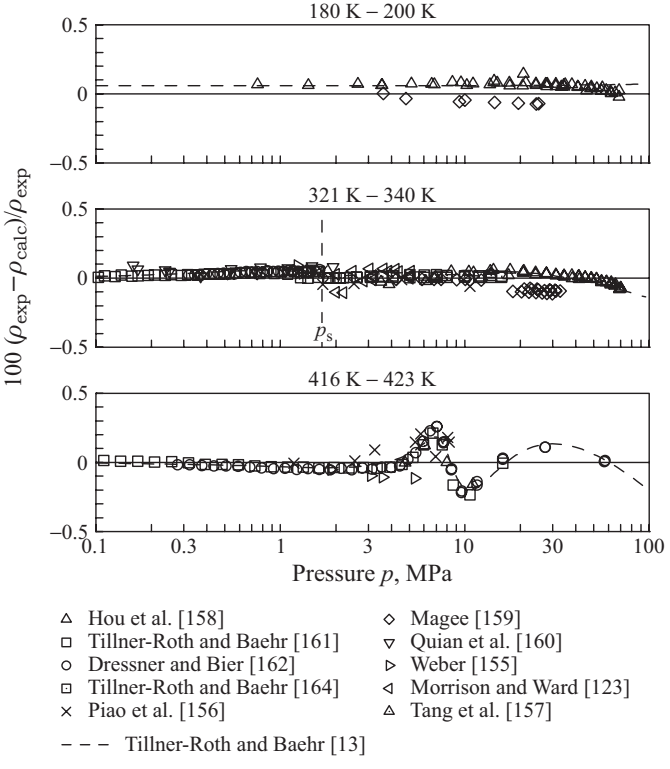

Fig. 9. Percentage deviations between selected experimental results for the density of HFC-134a and values calculated from the new equation of state, Eq. (2). Values calculated from the reference equation by Tillner-Roth and Baehr [13] are plotted for comparison.

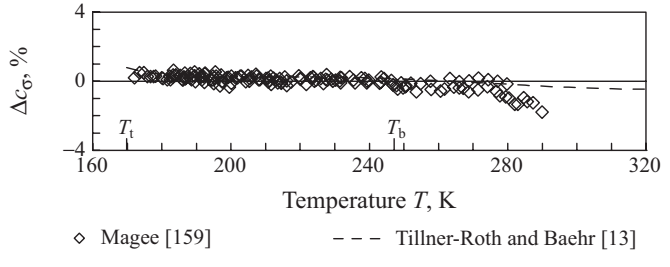

Fig. 10. Percentage deviations $\Delta c_\sigma, \% = 100(c_{\sigma,\mathrm{exp}} - c_{\sigma,\mathrm{calc}})/c_{\sigma,\mathrm{exp}}$ between selected experimental results for the saturated liquid heat capacity of HFC-134a and values calculated from the new equation of state, Eq. (2). Values calculated from the reference equation by Tillner-Roth and Baehr [13] are plotted for comparison.

Table XIV. Summary of the Data Sets Selected for HFC-143a and Average Absolute Deviations Between Values Calculated from the New Equation of State and the Selected Data

Authors	No. of data	Temperature and pressure range T (K)	p (MPa)	Average absolute deviations (AAD), % Gas	Liq.	Crit. reg.	Supercritical fluid LD[a]	MD[a]	HD[a]
***pρT* data**[b]									
Giuliani et al. [178]	14	274–364	0.6–0.8	0.043	–	–	0.126	–	–
Giuliani et al. [179]	61	268–364	0.5–4.1	0.130	–	0.145	0.080	–	–
Zhang et al. [180]	92	320–380	0.1–6.1	0.133	–	0.093	0.061	0.119	–
Weber and Defibaugh [181]	113	283–373	0.2–6.6	0.094	–	0.062	0.034	0.099	–
Defibaugh and Moldover [182]	624	243–323	1.5–6.5	–	0.049	–	–	–	–
DeVries [103], isochoric	500	243–393	1.5–18.1	–	0.074	0.066	0.092	0.160	0.022
DeVries [103], Burnett	529	263–433	0.0–20.6	0.038	–	0.080	0.030	0.152	0.103
Magee [183]	153	164–400	1.4–35.1	–	0.046	–	–	–	0.095
Isochoric heat capacities									
Magee [184]	149	173–342	3.1–34.0	–	0.402	–	–	–	–
Speeds of sound									
Gillis [147]	171	235–400	0.0–1.0	0.019	–	–	0.025	–	–
Saturated liquid heat capacities									
Magee [184]	90	165–341	Sat. liq.	–	0.376	–	–	–	–
Second virial coefficients									
Bignell and Dunlop [148]	3	290–310	–	0.421	–	–	–	–	–
Zhang et al. [180]	7	320–380	–	0.605	–	–	–	–	–
Beckermann and Kohler [185]	6	250–350	–	1.071	–	–	–	–	–
Gillis [147]	13	225–400	–	1.694	–	–	–	–	–

Authors	No of data	Temp. range T (K)	Average absolute deviations (AAD), % $T/T_c < 0.6$	$0.6 \leqslant T/T_c \leqslant 0.98$	$T/T_c > 0.98$
Vapor pressures[c]					
Russel et al. [186]	9	174–226	1.043	0.342	–
Weber and Defibaugh [181]	52	236–343	–	0.070	0.016
DeVries [103]	59	222–345	–	0.046	0.033
Saturated liquid densities					
Defibaugh and Moldover [182]	21	243–338	–	0.092	–

[a] LD: $\rho/\rho_c \leqslant 0.6$; MD: $0.6 < \rho/\rho_c < 1.5$; HD: $\rho/\rho_c \geqslant 1.5$.
[b] In the extended critical region, pressure deviations are given instead of density deviations.
[c] At temperatures $T/T_c < 0.6$, average absolute deviations in hPa are given.

3.11. Results for HFC-152a (1,1-Difluoroethane)

The data set which is available for the thermal properties of refrigerant HFC-152a covers the range from the triple-point temperature at $T_t \approx 154.6$ K ($T_t/T_c \approx 0.400$) to $T_{max} \approx 471$ K ($T_{max}/T_c \approx 1.22$) at pressures up to $p_{max} \approx 58$ MPa. Reliable experimental results are available for all

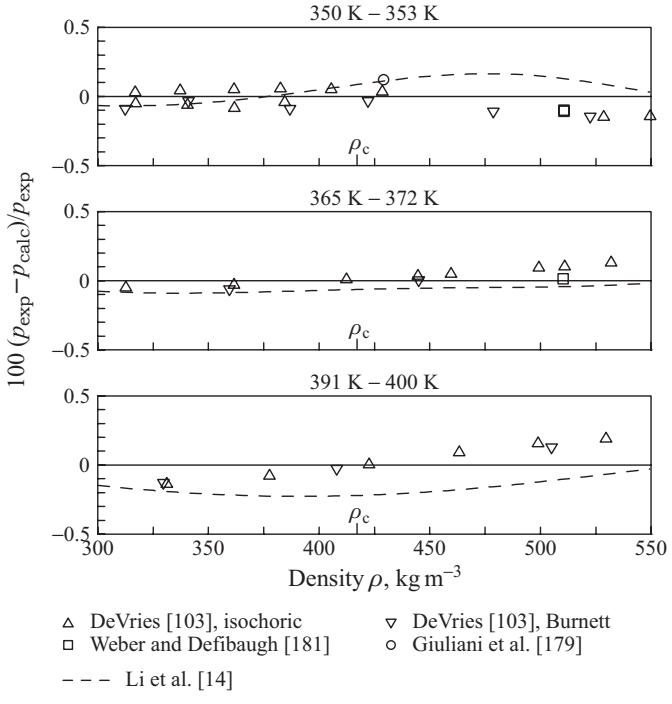

Fig. 11. Percentage pressure deviations between selected experimental results for the $p\rho T$ relation in the extended critical region of HFC-143a and values calculated from the new equation of state, Eq. (2). Values calculated from the equation by Li et al. [14] are plotted for comparison.

homogeneous states, for the vapor pressure, and for the saturated liquid density. Data for the saturated vapor density have been published for temperatures above 310 K, but the inconsistencies between different data sets exceed 2%. Accurate experimental information on the caloric properties of HFC-152a is scarce. Gas phase data are restricted to very low pressures. At liquid states, significant inconsistencies are observed between different sets of isobaric heat capacities. More detailed information on the available data set was published by Outcalt and McLinden [187]. Table XV summarizes the data sets selected for this project and gives percentage average absolute deviations between the selected experimental data and values calculated from the new equation of state, Eq. (2).

In general, the new equation of state for HFC-152a describes the selected data well within the uncertainties summarized in Table IV.

Table XV. Summary of the Data Sets Selected for HFC-152a and Average Absolute Deviations Between Values Calculated from the New Equation of State and the Selected Data

Authors	No. of data	Temperature and pressure range T (K)	p (MPa)	Average absolute deviations (AAD), % Gas	Liq.	Crit. reg.	Supercritical fluid LD[a]	MD[a]	HD[a]
***pρT* data**[b]									
Geller et al. [188]	49	247–471	1.3–57.9	–	0.049	–	–	–	0.043
Blanke and Weiß [189]	209	160–453	0.6–30.5	–	0.024	–	–	–	0.057
Tillner-Roth and Baehr [161]	335	293–433	0.1–16.3	0.021	–	0.083	0.031	0.198	0.074
Dressner and Bier [162]	149	333–423	0.2–57.6	0.026	–	0.076	0.056	0.274	0.149
Tillner-Roth and Baehr [164]	398	243–413	0.7–15.8	0.225	0.031	0.078	0.099	0.117	0.027
Speeds of sound									
Beckermann [168]	266	255–420	0.0–0.4	0.045	–	–	0.061	–	–
Hozumi et al. [190]	93	273–348	0.0–0.3	0.028	–	–	–	–	–
Kraft and Leipertz [191]	16	279–383	Saturated	0.541	0.985	–	–	–	–
Isobaric heat capacities									
Porichanskii et al. [192]	250	226–424	2.0–20.0	–	0.453	–	–	–	0.645
Benade [193]	17	243–323	3.0	–	0.454	–	–	–	–
Nakagawa et al. [194]	35[c]	276–360	1.0–3.2	–	0.310	–	–	–	–
Second virial coefficients									
Dressner and Bier [162]	4	333–423	–	0.311	–	–	–	–	–
Tillner-Roth and Baehr [161]	17	293–433	–	0.310	–	–	–	–	–

Authors	No of data	Temp. range T (K)	Average absolute deviations (AAD), % $T/T_c < 0.6$	$0.6 \leqslant T/T_c \leqslant 0.98$	$T/T_c > 0.98$
Vapor pressures[d]					
Higashi et al. [17]	44	273–386	–	0.077	0.063
Iso and Uematsu [195]	7	320–385	–	0.117	0.052
Baehr and Tillner-Roth [174]	57	301–386	–	0.076	0.047
Blanke and Weiß [189]	34	155–260	0.171	0.082	–
Tamatsu et al. [196]	46	320–386	–	0.053	0.040
Türk et al. [197]	41	208–386	0.192	0.062	0.168
Saturated liquid densities					
Geller et al. [188]	7	260–320	–	0.063	–
Higashi et al. [17]	6	371–386	–	0.073	1.912
Sato et al. [198]	5	223–273	0.082	0.081	–
Valtz et al. [199]	4	298–372	–	0.172	–
Baehr and Tillner-Roth [174]	13	243–353	–	0.025	–
Blanke and Weiß [189]	19	160–308	0.026	0.035	–
Holcomb et al. [110]	33	312–384	–	0.054	0.290

[a] LD: $\rho/\rho_c \leqslant 0.6$; MD: $0.6 < \rho/\rho_c < 1.5$; HD: $\rho/\rho_c \geqslant 1.5$.

[b] In the extended critical region, pressure deviations are given instead of density deviations.

[c] Published data adjusted according to $c_{p,\,cor} = 1.016 c_{p,\,exp}$ to increase the consistency of the c_p-data set.

[d] At temperatures $T/T_c < 0.6$, average absolute deviations in hPa are given.

Enlarged deviations up to $|\Delta\rho|/\rho \approx 0.4\%$ are observed only at supercritical states in the range of medium densities. However, in this range the corresponding deviations in pressure still remain within $|\Delta p|/p \leqslant 0.2\%$ and thus within the limit formulated for data in the extended critical region. As an example of the representation of thermal properties at the liquid-vapor phase equilibrium, Fig. 12 shows deviations between the selected data for the vapor pressure and the saturated liquid density of HFC-152a and values calculated from Eq. (2).

3.12. Results for Carbon Dioxide

The data set which was used for carbon dioxide covers the range from the triple-point temperature at $T_t \approx 216.6$ K ($T_t/T_c \approx 0.712$) to $T_{max} \approx 1024$ K ($T_{max}/T_c \approx 3.38$) at pressures up to $p_{max} = 100$ MPa. Accurate results are available for both thermal and caloric properties for all homogeneous states and on the vapor-liquid phase boundary, including highly accurate data for the saturated vapor density. However, except for isobaric heat capacities at low pressures, data for caloric properties are available

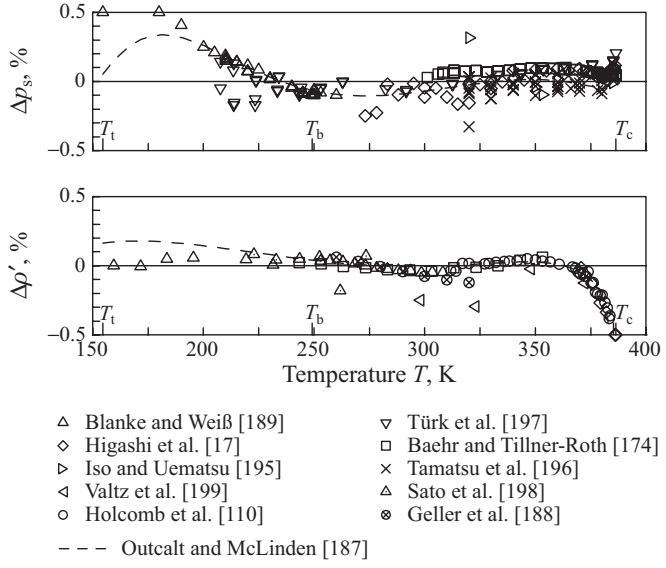

Fig. 12. Percentage deviations Δy, $\% = 100(y_{exp} - y_{calc})/y_{exp}$ with $y = p_s$ and ρ' between selected experimental results for the vapor pressure and the saturated liquid density of HFC-152a and values calculated from the new equation of state, Eq. (2). Values calculated from the reference equation by Outcalt and McLinden [187] are plotted for comparison.

Table XVI. Summary of the Data Sets Selected for Carbon Dioxide and Average Absolute Deviations Between Values Calculated from the New Equation of State and the Selected Data

Authors	No. of data	Temperature and pressure range T (K)	p (MPa)	Average absolute deviations (AAD), % Gas	Liq.	Crit. reg.	Supercritical fluid LD[a]	MD[a]	HD[a]
***pρT* data**[b]									
Michels et al. [200]	97[c]	273–423	12.3–96.7	–	0.140	0.087	–	0.140	0.137
Vukalovich and Altunin [201]	132	623–1024	1.1–59.0	–	–	–	0.175	0.617	–
Juza et al. [202]	13	323–498	70.0–100	–	–	–	–	–	0.199
Kirillin et al. [203]	39[c]	283–308	1.7–53.9	0.061	0.112	0.169	0.030	0.331	0.110
Kirillin et al. [204]	21[c]	433–473	2.0–57.8	–	–	–	0.051	0.250	–
Kirillin et al. [205]	97	313–413	1.7–53.4	–	–	0.085	0.078	0.162	0.078
Kirillin et al. [206]	24[c]	223–273	2.1–56.0	–	0.076	–	–	–	–
Popov and Sayapov [207]	41	223–303	12.9–30.0	–	0.063	–	–	–	–
Lau [208]	44[c]	240–350	12.7–69.5	–	0.120	–	–	0.122	0.114
Esper [209]	71	260–320	0.1–47.7	0.097	0.072	0.105	0.034	–	0.098
Holste et al. [210]	235	217–448	0.0–47.7	0.022	0.133	0.110	0.024	–	0.192
Jaeschke [211]	27	319–353	0.4–30.3	–	–	0.023	0.018	0.086	0.078
Jaeschke [212]	391	260–360	0.2–28.3	0.024	–	0.089	0.024	0.055	0.040
Magee and Ely [213]	9	250–330	5.8–27.1	–	0.091	0.131	–	–	0.026
Ely et al. [214]	55	250–330	2.2–35.5	0.069	0.087	0.097	0.103	0.240	0.053
Duschek et al. [215]	468	217–340	0.3–9.0	0.196	0.074	0.069	0.072	0.207	0.049
Jaeschke et al. [216][d]	123	273–320	0.2–10.5	0.013	–	0.076	0.011	0.045	–
Jaeschke et al. [216][e]	146	273–320	0.3–11.9	0.025	–	0.110	0.023	0.055	–
Gilgen et al. [217]	264	220–360	0.5–13.5	0.004	0.031	0.081	0.023	0.078	0.054
Guo et al. [218]	41	273–293	0.1–3.8	0.016	–	–	–	–	–
Brachthäuser et al. [219]	28	233–523	0.8–30.1	0.035	0.036	–	0.056	0.173	0.115
Fenghour et al. [220]	120	330–698	3.0–34.2	–	–	–	0.124	0.173	–
Nowak et al. [221]	21	313	8.4–12.1	–	–	0.136	–	0.041	0.075
Klimeck et al. [222]	73	300–430	0.5–30.1	0.023	0.061	–	0.032	0.164	0.065
Isochoric heat capacities									
Magee and Ely [223]	69	233–331	7.4–32.2	–	1.128	2.859	–	–	0.533
Abdulagatov et al. [224]	30	317–357	9.6–16.8	–	–	2.497	–	2.679	–
Speeds of sound									
Novikov and Trelin [225]	11[c]	278–300	Sat. vap.	0.765	–	–	–	–	–
Novikov and Trelin [226]	234	288–373	2.9–9.8	0.478	–	0.978	0.187	0.450	0.447
Pecceu and van Dael [227]	23	217–294	Sat. liq.	–	0.696	–	–	–	–
Lemming [84]	50	240–360	0.3–0.9	0.015	–	–	0.005	–	–
Isobaric/saturated liquid heat capacities									
Bender et al. [228]	60[c]	233–473	0.1–1.5	0.646	–	–	0.117	–	–
Magee and Ely [223]	77	220–303	Sat. liq.	–	0.688	2.325	–	–	–
Ernst et al. [229]	55	333–393	0.2–89.7	–	–	0.375	0.412	0.657	0.403
Ernst and Hochberg [230]	9	303	0.3–52.2	0.299	0.742	–	–	–	–
Enthalpy differences									
Möller et al. [231]	10	233–358	14.6–15.7	–	0.797	–	–	0.372	0.259
Joule-Thomson coefficients									
Bender et al. [228]	35	233–473	0.2–1.5	1.058	–	–	0.476	–	–

Table XVI. *(Continued)*

Authors	No of data	Temp. range T (K)	Average absolute deviations (AAD), % $T/T_c < 0.6$	$0.6 \leqslant T/T_c \leqslant 0.98$	$T/T_c > 0.98$
Vapor pressures[e]					
Duschek et al. [232]	110	217–304	–	0.062	0.058
Saturated liquid densities					
Duschek et al. [232]	47	217–304	–	0.070	0.431
Saturated vapor densities					
Duschek et al. [232]	42	217–304	–	0.070	1.664

[a] LD: $\rho/\rho_c \leqslant 0.6$; MD: $0.6 < \rho/\rho_c < 1.5$; HD: $\rho/\rho_c \geqslant 1.5$.
[b] In the extended critical region, pressure deviations are given instead of density deviations.
[c] Adjusted data used; see Ref. 18.
[d] Burnet measurements.
[e] Refractive-index measurements.
[f] Due to the high triple-point temperature no data are available at $T/T_c < 0.6$.

only up to $T \approx 393$ K ($T/T_c \approx 1.29$). Characteristic features of the data set for carbon dioxide are an experimentally well described extended critical region and data that are available up to much higher reduced temperatures than for the other polar fluids considered. An extensive review on the available data set was published by Span and Wagner [18]. Table XVI summarizes the data sets selected for this project and gives percentage average absolute deviations between the selected experimental data and values calculated from the new equation of state, Eq. (2).

In general, the new equation of state represents the reliable experimental results for the thermodynamic properties of carbon dioxide well within the demanded uncertainties. Figure 13 shows a comparison between experimental data for caloric properties on the vapor-liquid phase boundary and values calculated from Eq. (2). As for HFC-125 (see Section 3.8), speeds of sound in the saturated liquid and vapor are represented within $|\Delta w|/w \leqslant 2\%$ up to reduced temperatures of $T/T_c \approx 0.96$ and $T/T_c \approx 0.99$, respectively. Experimental results for the heat capacity of the saturated liquid are represented within $|\Delta c_\sigma|/c_\sigma \leqslant 2\%$ up to $T/T_c \approx 0.99$. For a technical equation of state, these results are considered to be excellent.

Figure 14 shows deviations between experimental data for the $p\rho T$ relation and values calculated from Eq. (2). At gaseous, liquid, and typical supercritical states, the experimental results are represented well within the limits defined in Table IV. However, at temperatures above $T \approx 400$ K and pressures above $p \approx 20$ MPa, increased deviations are observed. Up to $T \approx 600$ K these deviations stay within $|\Delta\rho|/\rho \leqslant \approx 0.4\%$; at higher temperatures, they increase up to $|\Delta\rho|/\rho \approx 1\%$. At high reduced temperatures,

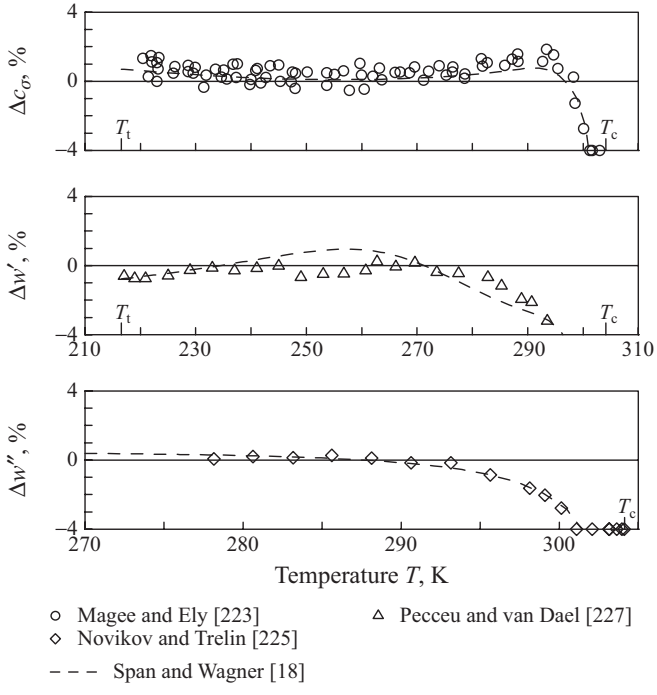

Fig. 13. Percentage deviations $Dy,\% = 100(y_{exp} - y_{calc})/y_{exp}$ with $y = c_\sigma$, w', and w'' between selected experimental results for caloric properties on the phase boundary of carbon dioxide and values calculated from the new equation of state, Eq. (2). Values calculated from the reference equation by Span and Wagner [18] are plotted for comparison.

the simultaneous optimization procedure used to develop the functional form of Eq. (2) had to rely exclusively on data for carbon dioxide; see also Ref. 2. No reliable data were available for the other polar fluids at reduced temperatures above $T/T_c \approx 1.42$. Based only on high temperature data for carbon dioxide, the simultaneous optimization algorithm did not find functional forms which improve the representation of $p\rho T$ data at high (reduced) temperatures and high pressures without affecting the average quality of the resulting equations of state. To overcome this problem, high-temperature data for thermodynamic properties of other polar fluids would be required.

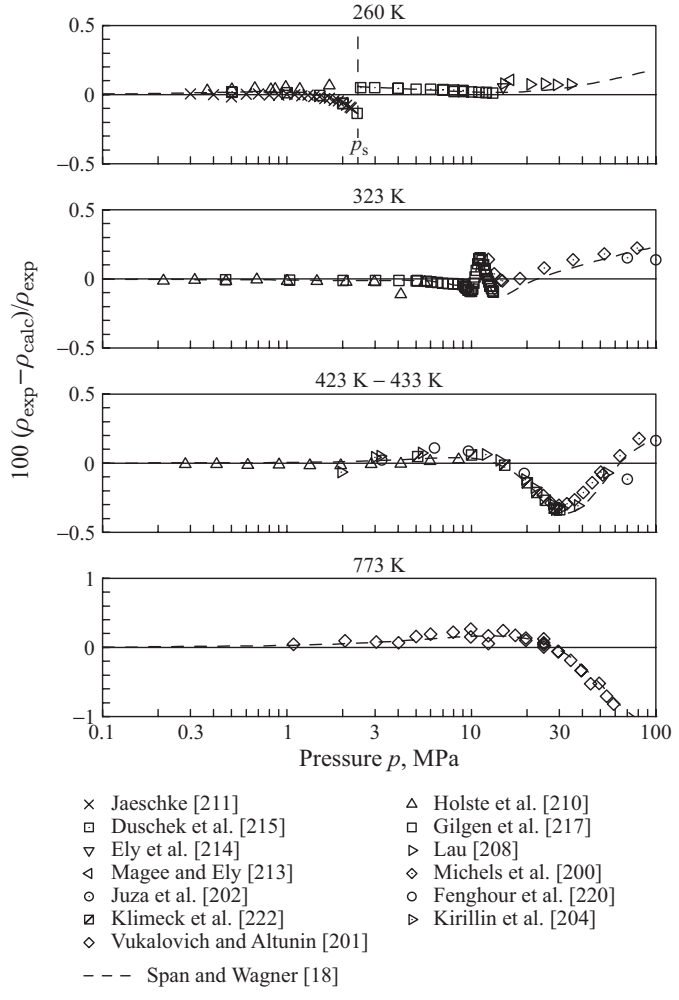

Fig. 14. Percentage deviations between selected experimental results for the density of carbon dioxide and values calculated from the new equation of state, Eq. (2). Values calculated from the reference equation by Span and Wagner [18] are plotted for comparison.

3.13. Results for Ammonia

The data set used for ammonia covers the temperature range from the triple-point temperature at $T_t \approx 195.5$ K ($T_t/T_c \approx 0.482$) to $T_{max} \approx 574$ K ($T_{max}/T_c \approx 1.42$) at pressures up to $p_{max} \approx 85$ MPa. For thermal properties,

Table XVII. Summary of the Data Sets Selected for Ammonia and Average Absolute Deviations Between Values Calculated from the New Equation of State and the Selected Data

Authors	No. of data	Temperature and pressure range T (K)	p (MPa)	Average absolute deviations (AAD), % Gas	Liq.	Crit. reg.	Supercritical fluid LD[a]	MD[a]	HD[a]
***pρT* data**[b]									
Meyers and Jessup [233]	49	278–573	0.1–2.9	0.033	–	–	0.047	–	–
Beatie and Lawrence [234]	37	323–398	1.5–6.9	0.092	–	–	–	–	–
Kumagai and Toriumi [235]	14	253–313	38.2–85.3	–	0.128	–	–	–	–
Date [236]	74	405–407	11.0–11.9	–	–	0.128	–	–	–
Garnjost [237]	147	333–574	5.0–72.3	0.132	0.043	0.088	0.227	0.382	0.112
Zander and Thomas [238]	22	224–338	4.5–37.3	–	0.044	–	–	–	–
Streatfield and Henderson [239]	14	195–290	0.0–0.8	–	0.084	–	–	–	–
Glowka [240]	47	298–473	0.2–6.0	0.041	–	–	0.066	–	–
Harms-Watzenberg [241]	418	243–413	0.8–39.5	0.271	0.043	0.058	0.095	0.337	0.044
Speeds of sound									
Blagoi et al. [242]	10	200–270	0.0–0.4	–	3.142	–	–	–	–
Isobaric/saturated liquid heat capacities									
Osborne and van Dusen [243]	50	227–319	Sat. liq.	–	0.457	–	–	–	–
Osborne et al. [244]	64	258–423	0.1–2.0	0.683	–	–	0.144	–	–
Overstreet and Giauque [245]	18	198–240	Sat. liq.	–	1.530	–	–	–	–
Second virial coefficients									
Hirschfelder et al. [41]	3	473–573	–	1.241	–	–	–	–	–
Glowka [240]	9	298–473	–	1.065	–	–	–	–	–

Authors	No of data	Temp. range T (K)	Average absolute deviations (AAD), % $T/T_c < 0.6$	$0.6 \leqslant T/T_c \leqslant 0.98$	$T/T_c > 0.98$
Vapor pressures[c]					
Cragoe et al. [246]	145	220–343	0.678	0.088	–
Stock et al. [247]	35	204–238	0.295	–	–
Beattie and Lawrence [234]	14	303–405	–	0.252	0.075
Garnjost [237]	16	328–404	–	0.184	0.054
Saturated liquid densities					
Cragoe and Harper [248]	88	195–373	0.020	0.052	–
Groenier and Thodos [249]	4	243–345	–	0.076	–
Streatfield and Henderson [239]	24	200–284	0.086	0.039	–
Harms-Watzenberg [241]	11	243–373	0.027	0.054	–
Saturated vapor densities					
Cragoe et al. [250]	77[d]	222–323	0.796	0.326	–

[a] LD: $\rho/\rho_c \leqslant 0.6$; MD: $0.6 < \rho/\rho_c < 1.5$; HD: $\rho/\rho_c \geqslant 1.5$.
[b] In the extended critical region, pressure deviations are given instead of density deviations.
[c] At temperatures $T/T_c < 0.6$, average absolute deviations in hPa are given.
[d] Data used with reduced weighting factors due to a large, experimentally caused scatter.

the available data set is extensive, but reliable experimental results for caloric properties are available only at pressures up to $p \approx 2$ MPa. Most of the data are rather old, and only few data sets satisfy current scientific demands on accuracy. However, for the development of a technical equation of state, the data situation is satisfactory. A brief review of the available data set was published by Tillner-Roth *et al.* [19]. Table XVII summarizes the data sets selected for this project and gives percentage average absolute deviations between the selected experimental data and values calculated from the new equation of state, Eq. (2).

In general, the new equation of state represents the available data within the demanded uncertainties up to $T \approx 430$ K ($T/T_c \approx 1.06$). Slightly larger deviations up to $\Delta p_s/p_s \approx 0.25\%$ are found for vapor pressures at temperatures between 330 K and 370 K. At very low temperatures,

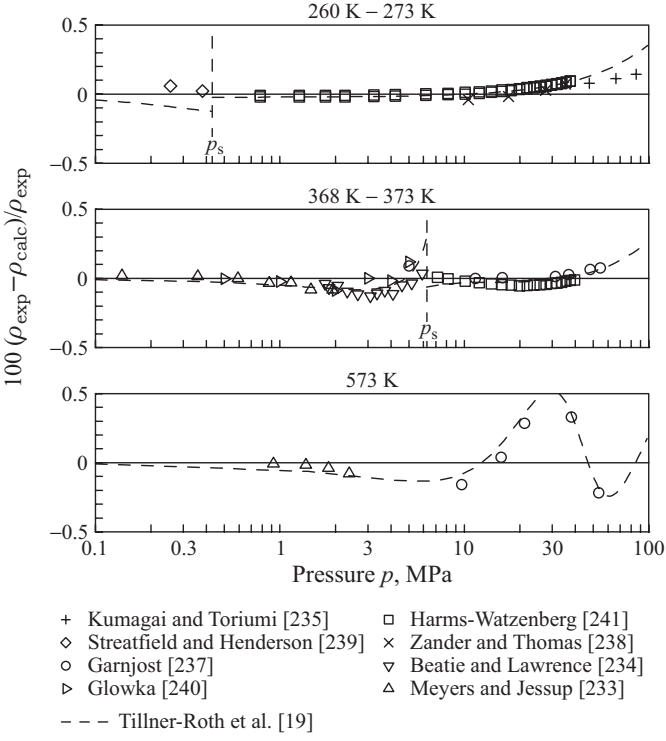

Fig. 15. Percentage deviations between selected experimental results for the density of ammonia and values calculated from the new equation of state, Eq. (2). Values calculated from the reference equation by Tillner-Roth et al. [19] are plotted for comparison.

deviations up to $\Delta w/w \approx -5\%$ are observed for the liquid-phase speed of sound data by Blagoi et al. [242]. However, these data seem to be inconsistent with the saturated liquid heat capacity data available in the same range of temperatures.

At temperatures above 430 K and pressures above ≈ 10 MPa, larger deviations on the order of $|\Delta\rho|/\rho \approx 0.5\%$ are observed between calculated densities and the $p\rho T$ data published by Garnjost [237]. Figure 15 illustrates both the good representation of $p\rho T$ data at gaseous and liquid states and the shortcomings observed at high temperatures. The enlarged deviations which occur at much lower reduced temperatures than those observed for other fluids are attributed to the fact that the thermodynamic property surface of ammonia is significantly influenced by association. The functional form of Eq. (2) was not primarily optimized for the description of associating fluids; see Ref. 2. Thus, the fact that a fluid like ammonia can be described quite accurately with this functional form is considered a very positive result. However, applied to strongly associating fluids like water, Eq. (2) yields unsatisfactory results; see also Section 4.

4. SUMMARY AND PROSPECTS

Based on the simultaneously optimized functional form for polar fluids presented in Ref. 2, state-of-the-art technical equations of state have been developed for 12 fluids. A total of 22,528 selected data points from more than 220 references has been used to fit and evaluate these equations. The results of comparisons with the selected data are summarized in Tables VI to XVII. The number of data points which have not been selected for different reasons and which are thus not documented here was of the same order. It has been shown that the simultaneously optimized functional form presented in Ref. 2 is suitable for a sufficiently accurate description of a broad variety of fluids with very different polarity. On average, the new equations are far superior to older technical equations of state. In many cases, their performance comes close to the performance of typical reference equations. During our work on the equations presented in this article, limitations of the new functional form for polar fluids became obvious with regard to the accurate description of supercritical states at high reduced temperatures and high pressures, and with regard to the description of associating fluids.

To establish a simultaneously optimized functional form which yields a better representation of supercritical states at high reduced temperatures and high pressures, data at such states would be required for additional polar fluids. However, most of the technically relevant polar fluids are

chemically unstable at these conditions. Thus, it is questionable whether such data will ever become available. On the other hand, this means that the observed shortcomings are not relevant for typical technical applications. Investigations of ideal curves and absolute plots of different properties show that a qualitatively correct extrapolation behavior which may be relevant for applications of the new equations of state in mixture models can be assumed up to very high reduced temperatures and pressures.

It is not yet clear whether strongly associating fluids like water or alcohols can simply be treated as a further group of fluids or whether they can be accurately described by adding some kind of association term to the functional form developed for non associating fluids. First attempts to add such a term to Eq. (2) showed some success [251], but the demands on accuracy formulated in Table IV are still unattainable.

Multiparameter equations of state were previously available for all of the fluids discussed here. The upcoming challenge is to describe fluids with this new class of accurate and numerically stable equations of state which have not yet been described with multiparameter equations at all. Equations of state for other fluids belonging to the group of polar fluids are being developed and will be published in further articles of this series. Software for fitting equations of state based on the new functional form can be made available to other scientists who want to use their own data sets as input.

ACKNOWLEDGMENTS

The authors are indebted to the Deutsche Forschungsgemeinschaft for their financial support and to Prof. R. T Jacobsen and Dr. E. W. Lemmon, whose literature database *BIBLIO* was very helpful for setting up the required data sets.

REFERENCES

1. R. Span, H.-J. Collmann, and W. Wagner, *Int. J. Thermophys.* **19**:491 (1998).
2. R. Span and W. Wagner, *Int. J. Thermophys.* **24**:1 (2003).
3. R. Span and W. Wagner, *Int. J. Thermophys.* **24**:41 (2003).
4. R. Span, *Multiparameter Equations of State—An Accurate Source of Thermodynamic Property Data* (Springer, Berlin, 2000).
5. V. Marx, A. Pruß, and W. Wagner, *Neue Zustandsgleichungen für R-12, R-22, R-11 und R-113, Beschreibung des thermodynamischen Zustandsverhalten bei Temperaturen bis 525 K und Drücken bis 200 MPa,* Fortschr.-Ber. VDI, Reihe **6**, 57 (1992).
6. W. Wagner, V. Marx, and A. Pruß, *Rev. Int. Froid* **16**:373 (1993)
7. R. Tillner-Roth and A. Yokozeki, *J. Phys. Chem. Ref. Data* **26**:1273 (1997).
8. S. L. Outcalt and M. O. McLinden, *Int. J. Thermophys.* **16**:79 (1995).

9. B. A. Younglove and M. O. McLinden, *J. Phys. Chem. Ref. Data* **23**:731 (1994).
10. S. Tanikawa, Y. Kabata, H. Sato, and K. Watanabe, *J. Chem. Eng. Data* **35**:381 (1990).
11. M. Fukushima, N. Watanabe, and T. Kamimura, *Trans. JAR* **7**:85 (1990).
12. C. C. Piao and M. Noguchi, *J. Phys. Chem. Ref. Data* **27**:775 (1998).
13. R. Tillner-Roth and H. D. Baehr, *J. Phys. Chem. Ref. Data* **23**:657 (1994).
14. J. Li, R. Tillner-Roth, H. Sato, and K. Watanabe, *Int. J. Thermophys.* **20**:1639 (1999).
15. J. Li, R. Tillner-Roth, H. Sato, and K. Watanabe, *An Equation of State for 1,1,1-Trifluoroethane (R-143a)*, in W. M. Haynes, ed., *Proc. of the 13th Symp. on Thermophys. Prop.*, Preprint Volume (Boulder, Colorado, 1997).
16. R. Tillner-Roth, *Int. J. Thermophys.* **16**:91 (1995).
17. Y. Higashi, M. Ashizawa, Y. Kabata, T. Majima, M. Uematsu, and K. Watanabe, *JSME Int. J.* **30**:1106 (1987).
18. R. Span and W. Wagner, *J. Phys. Chem. Ref. Data* **25**:1509 (1996).
19. R. Tillner-Roth, F. Harms-Watzenberg, and H. D. Baehr, *Eine neue Fundamentalgleichung für Ammoniak,* DKV-Tagungsber. **20** (DKV, Stuttgart, 1993).
20. H. Preston-Thomas, *Metrologia* **12**:7 (1990).
21. R. L. Rusby, *J. Chem. Thermodyn.* **23**:1153 (1990).
22. T. B. Coplen, *J. Phys. Chem. Ref. Data* **26**:1239 (1997).
23. E. R. Cohen and B. N. Taylor, *J. Phys. Chem. Ref. Data* **17**:1795 (1988).
24. P. J. Mohr and B. N. Taylor, *J. Phys. Chem. Ref. Data* **28**:1713 (1999).
25. R. T Jacobsen, S. G. Penoncello, and E. W. Lemmon, *Fluid Phase Equil.* **80**:45 (1992).
26. A. F. Benning and R. C. McHarness, *Ind. Eng. Chem.* **32**:698 (1940).
27. E. A. Kremenevskaya and S. L. Rivkin, *Teplofiz. Svoj. Ves. Material.* **8**:46 (1975).
28. S. L. Rivkin and E. A. Kremenevskaya, *Thermophys. Prop. Matter Substance* **8**:1 (1975).
29. V. P. Kolebev and A. M. Shaemardanov, *Experimental Investigation of Refractive Index of freon-11.* Deposited in VINITI, Doc.-No.: 3592-80 (1980).
30. W. Blanke, *pvT-Measurements for R-11.* Private communication, PTB, Braunschweig (1988).
31. W. Blanke, *pvT Measurements for R-12, R-11, and R-113.* Private communication, PTB, Braunschweig (1989).
32. W. Blanke, *pvT-Measurements for R-11 and R-113.* Private communication, PTB, Braunschweig (1989).
33. W. Blanke and R. Weiß, *PTB-Mitteilungen* **107**:115 (1997).
34. L. Kolomov, A. K. Solov'ev, and E. P. Sheludyakov, *Zh. Prikl. Mekh. Tekh. Fiz.* **3**:141 (1968).
35. K. J. Meyer, *Kältetechnik–Klimatisierung* **21**:270 (1969).
36. M. Chavez, P. Habichayn, and R. Tsumura, *J. Chem. Eng. Data* **31**:218 (1986).
37. A. Lainez, P. Gopal, A. Zollweg, and W. B. Street, *J. Chem. Thermodyn.* **21**:773 (1989).
38. D. W. Osborne, C. S. Garner, R. N. Doescher, and D. M. Yost, *J. Am. Chem. Soc.* **63**:3496 (1941).
39. A. Ya. Grishkov and A. M. Sirota, *Thermophys. Prop. Matter Substance* **4**:34 (1971).
40. H. Wirbser, G. Bräuning, and G. Ernst, *J. Chem. Thermodyn.* **24**:783 (1992).
41. J. O. Hirschfelder, F. T. McClure, and I. F. Weeks, *J. Chem. Phys.* **10**:201 (1942).
42. L. Riedel, *Z. ges. Kälteindustrie* **46**:197 (1939).
43. E. A. Kremenevskaya and S. L. Rivkin, *Teplofiz. Svoj. Ves. Material.* **8**:40 (1975).
44. E. Fernandez-Fassnacht and F. Del Rio, *J. Chem. Thermodyn.* **16**:1003 (1984).
45. A. F. Benning and R. C. McHarness, *Ind. Eng. Chem.* **32**:814 (1940).
46. M. Kriebel and H. J. Löffler, *Kältetechnik–Klimatisierung* **18**:34 (1966).
47. M. Okada, M. Uematsu, and K. Watanabe, Measurements of saturated liquid density for several refrigerants, in *Proc. 16th Int. Cong. Refrigeration* (Int. Inst. Refrig., Paris, 1983).

48. M. Okada, M. Uematsu, and K. Watanabe, *J. Chem. Thermodyn.* **18**:527 (1986).
49. G. Händel, R. Kleinrahm, and W. Wagner, *J. Chem. Thermodyn.* **24**:697 (1992).
50. S. G. Penoncello, R. T Jacobsen, and E. W. Lemmon, *Fluid Phase Equil.* **80**:57 (1992).
51. A. Michels, T. Wassenaar, G. J. Wolkers, Chr. Prins, and L. van der Klundert, *J. Chem. Eng. Data* **11**:449 (1966).
52. I. I. Perel'shtein, *Thermophys. Prop. Matter Substance* **2**:225 (1970).
53. K. Watanabe, T. Tanaka, and K. Oguchi, Compressibility and virial coefficients of dichlorodifluoromethane (R-12) with Burnett apparatus, in *Proc. 7th Symp. Thermophys. Prop.* (ASME, New York, 1977).
54. A. Kumagi and H. Iwasaki, *J. Chem. Eng. Data* **23**:193 (1978).
55. K. Oguchi, Y. Takaishi, and I. Tanishita, *Trans. JSME B* **50**:2606 (1984).
56. G. A. Iglesias-Silva, *pvT measurements for R-12*. Private communication, (Texas A&M University, College Station, 1987). Data partly published in: R. C. Castro-Gomez, G. A. Igelsias-Silva, W. R. Lau, J. C. Holste, K. N. Marsh, K. R. Hall, and P. T. Eubank, *Experimental Enthalpies and Densities of Compressed Liquid Refrigerants.* Paper 85-WA/HT-57, (ASME, New York, 1986).
57. W. Blanke, H. Häusler, and R. Weiß, *PTB-Mitteilungen* **98**:253 (1988).
58. W. Blanke, *pvT Measurements for R-12 and R-22*. Private communication, (PTB, Braunschweig, 1989).
59. Y. Hwang, *The Constant Volume Heat Capacities of Gaseous Tetrafluoromethane, Chlorodifluoromethane, Dichlorotetrafluoroethane and Chloropenta-Fluoro-Ethane* (Ph.D. Thesis, University of Michigan, Ann Arbor, 1961).
60. J. Woodburn, M. T. Mettrey, and B. L. Hoa, *ASHRAE J.* **8**:74 (1966).
61. E. P. Sheludyakov, Yu. L. Kolotov, and A. N. Solov'ev, *Teplofiz. Svojstva Frenov* **96** (1969).
62. G. R. Poole and R. A. Aziz, *AIChE J.* **18**:430 (1972).
63. W. S. Winters, Jr. and H. Merte, Jr., *J. Appl. Phys.* **48**:3605 (1977).
64. A. C. Tam and W. P. Leung, *Phys. Rev. Let.* **53**:560 (1984).
65. J. F. Masi, *J. Am. Chem. Soc.* **74**:4738 (1952).
66. R. C. McHarness, B. J. Eisemann, and J. J. Martin, *Refrig. Eng.* **63**:31 (1955).
67. G. Ernst, *Chemie-Ing.-Techn.* **41**:544 (1969).
68. V. A. Gruzdev and A. I. Shumskaya, *Thermophys. Prop. Matter Substance* **8**:108 (1975).
69. R. C. Castro-Gomez, *A Thermodynamic Total Enthalpy Flow Calorimeter: Its Application to Binary Mixtures of Chlorofluoromethanes* (Ph.D. Thesis, Texas A&M University, College Station, 1987).
70. B. Schramm, *Measurements of 2nd Virial Coefficients of R-12 and R-22,* Private communication (University Heidelberg, Heidelberg, 1988).
71. K. Oguchi, Y. Takaishi, and I. Tanishita, Experimental study of pressure-volume-temperature relationships for dichlorodifluoromethane (R-12) in *Proc. 16th Int. Congr. Refrig.,* Vol. 2, (Paris, 1983).
72. W. Blanke and R. Weiß, *Vapor-Pressure Measurements for R-12 and R-22*. Private communication, (PTB, Braunschweig, 1990).
73. A. Kamei, S. W. Beyerlein, and R. T Jacobsen, *Int. J. Thermophys.* **16**:1155 (1995).
74. A. Michels, *pvT Data for R-22,* in J. J. Martin, ed., *Ind. Eng. Chem.* **59**:34 (1967).
75. A. V. Kletskii, *Teplofiz. Sovo. Freona-22* (Komitet Standartov, Moskva, 1970).
76. K. Oguchi, H. Sagara, I. Matsushita, K. Watanabe, and I. Tanishita, *Trans. Jap. Soc. Mech. Eng.* **45**:1522 (1979).
77. R. Kohlen, H. Kratzke, and S. Müller, *J. Chem. Thermodyn.* **17**:1141 (1985).
78. R. Kohlen, *Das fluide Zustandsgebiet von R-22*. Fortschr.-Ber. VDI, Reihe 19, 14 (1987).

79. W. Blanke and R. Weiß, *Messungen der Druck-Temperaturabhängigkeit der Flüssigkeitsdichten von Chlordifluormethan (R-22) vom Tripelpunkt bis 400 K.* DKV-Tagungsber., Vol. 17 (DKV, Stuttgart, 1990).
80. H. Fukuizumi and M. Uematsu, *J. Chem. Eng. Data* **36**:91 (1991).
81. V. G. Niesen, L. J. van Poolen, S. L. Outcalt, and C. D. Holcomb, *Fluid Phase Equil.* **97**:81 (1994).
82. I. I. Novikov and L. M. Lagutina, *Zh. Prikl. Mekh. Fiz.* **8**:147 (1967).
83. R. Niepmann, *Messung der Ultraschallgeschwindigkeit in Flüssigkeiten über einen großen Temperatur- und Druckbereich* (Ph.D. Thesis, Ruhr-University Bochum, 1983).
84. W. Lemming, *Experimentelle Bestimmung akustischer und thermischer Virialkoeffizienten von Arbeitsstoffen der Energietechnik,* Fortschr.-Ber. VDI, Reihe 19, 32 (1989).
85. E. F. Neilson and D. White, *J. Am. Chem. Soc.* **79**:5618 (1957).
86. G. Ernst and J. Büsser, *J. Chem. Thermodyn.* **2**:787 (1970).
87. K. Bier, G. Ernst, and G. Maurer, *J. Chem. Thermodyn.* **6**:1027 (1974).
88. G. Ernst and H. Wirbser, *Isobaric Heat Capacities of R-22*, Private communication (University Karlsruhe, Karlsruhe, 1991).
89. K. Bier, G. Maurer, and H. Sand, *Ber. Bunsenges. Phys. Chem.* **84**:430 (1980).
90. R. Günther and K. Stephan, *Klima-Kälte-Heizung* **17**:242 (1989).
91. R. Günther and K. Stephan, *Klima-Kälte-Heizung* **17**:292 (1989).
92. B. Schramm and Ch. Weber, *J. Chem. Thermodyn.* **23**:281 (1991).
93. M. Kriebel, *Kältetechnik-Klimatisierung* **19**:8 (1967).
94. Y. Takaishi, N. Kagawa, M. Uematsu, and K. Watanabe, Volumetric properties of the binary mixtures dichlorodifluoromethane + chlorodifluoromethane, in *Proc. 8th Symp. on Thermophys. Prop.,* Vol. 2 (ASME, New York, 1982), pp. 387–395.
95. H. Fukuizima and M. Uematsu, *Int. J. Thermophys.* **12**:371 (1991).
96. J. C. Holste, H. A. Duarte-Garza, and M. A. Villamanan-Olfos, *Thermodynamic Properties Measurements* (ASME Winter Annual Meeting, New Orleans, Louisiana, 1993).
97. Z. Y. Quian, H. Nishimura, H. Sato, and K. Watanabe, *Int. J. JSME B* **36**:665 (1993).
98. C. Bouchon and D. Richon, Simultaneous measurements of phase equilibrium and volumetric properties by vibrating tube densimetry: apparatus and results involving HFC, in *Proc. Joint Meeting IIR Com. B1, B2, E1, and E2* (Padova, Italy, 1994).
99. D. R. Defibaugh, G. Morrison, and L. A. Weber, *J. Chem. Eng. Data* **39**:333 (1994).
100. T. Sato, H. Sato, and K. Watanabe, *J. Chem. Eng. Data* **39**:851 (1994).
101. J. W. Magee, *Int. J. Thermophys.* **17**:803 (1996).
102. H.-L. Zhang, H. Sato, and K. Watanabe, *J. Chem. Eng. Data* **41**:1401 (1996).
103. B. deVries, *Thermodynamische Eigenschaften der Kältemittel R-32, R-125 und R-143a,* DKV-Forsch.-Ber. 55 (DKV, Stuttgart, 1997).
104. T. O. D. Lüddecke and J. W. Magee, *Int. J. Thermophys.* **17**:823 (1996).
105. A. J. Grebenkov, Y. G. Kotelevsky, V. V. Saplitza, O. V. Beljaeva, T. A. Zajatz, and B. D. Timofeev, Experimental study of thermal conductivity of some ozone safe refrigerants and speed of sound in their liquid phase, in *Proc. Joint Meeting IIR Com. B1, B2, E1, and E2* (Padova, Italy, 1994).
106. T. Hozumi, H. Sato, and K. Watanabe, *J. Chem. Eng. Data* **39**:493 (1994).
107. M. Yomo, H. Sato, and K. Watanabe, *High Temp.–High Press.* **26**:267 (1994).
108. P. F. Malbrunot, P. A. Meunier, G. M. Scatena, W. H. Mears, K. P. Murphy, and J. V. Sinka, *J. Chem. Eng. Data* **13**:16 (1968).
109. A. Kanungo, T. Oi, A. Popowicz, and T. Ishida, *J. Phys. Chem.* **91**:4198 (1987).
110. C. D. Holcomb, V. G. Niesen, L. J. van Poolen, and S. L. Outcalt, *Fluid Phase Equil.* **91**:145 (1993).

111. L. A. Weber and A. R. H. Goodwin, *J. Chem. Eng. Data* **38**:254 (1993).
112. L. A. Weber and A. M. Silva, *J. Chem. Eng. Data* **39**:808 (1994).
113. M. Nagel and K. Bier, *Int. J. Refrig.* **18**:534 (1995).
114. L. Riedel, *Z. ges. Kälteindustrie* **45**:221 (1938).
115. V. Z. Geller, *Teplofiz. Svoj. Ves. Material.* **7**:135 (1973).
116. M. J. Mastroianni, R. F. Stahl, and P. N. Sheldon, *J. Chem. Eng. Data* **23**:113 (1978).
117. Yu. A. Vesloguzov, *Teplofiz. Svoj. Ves. Material.* **13**:42 (1979).
118. O. P. Ponomareva, *Teplofiz. Svoj. Ves. Material.* **16**:64 (1982).
119. R. M. Varushenko and L. L. Bulgatova, *Trudy Chim. Chim. Technol.* **1**:69 (1974).
120. N. Matsuo, Thermophysical properties of R-123, pvT properties, viscosity, and thermal conductivity, in *Proc. 9th Japan Symp. Thermophys. Prop.* (1988), pp. 231–234.
121. Y. Maezawa, H. Sato, and K. Watanabe, *J. Chem. Eng. Data* **35**:225 (1990).
122. L. A. Weber, *J. Chem. Eng. Data* **35**:237 (1990).
123. G. Morrison and D. K. Ward, *Fluid Phase Equil.* **62**:65 (1991).
124. C. C. Piao, H. Sato, and K. Watanabe, *J. Chem. Eng. Data* **36**:398 (1991).
125. K. Oguchi, M. Yamagishi, and A. Murano, *Fluid Phase Equil.* **80**:131 (1992).
126. J. W. Magee, *Int. J. Thermophys.* **21**:1303 (2000).
127. J. W. Magee, *Int. J. Thermophys.* **21**:1291 (2000).
128. A. R. H. Goodwin and M. R. Moldover, *J. Chem. Phys.* **95**:5236 (1991).
129. T. Takagi, *J. Chem. Eng. Data* **36**:394 (1991).
130. N. Nakagawa, H. Sato, and K. Watanabe, *J. Chem. Eng. Data* **36**:156 (1991).
131. T. Yamashita, H. Kubota, Y. Tanaka, T. Makita, and H. Kashiwagi, Physical properties of new halogenated hydrocarbons, in *Proc. 10th Japan Symp. Thermophys. Prop.* (1989).
132. M. Buschmeier, W. Künstler, G. Herres, and D. Gorenflo, *Phasengleichgewicht und Dichte der Stoffsysteme R-22/R-142b sowie R-227/R-123.* DKV-Tagungsber. **19** (DKV, Stuttgart, 1992).
133. L. A. Weber, *Fluid Phase Equil.* **80**:141 (1992)
134. K. Oguchi and Y. Takaishi, Measurement of saturated liquid density of HCFC-123, in *Proc. 10th Japan Symp. Thermophys. Prop.* (1989).
135. J. Schmidt, *Saturated Liquid Densities for R 123,* Private communication, (NIST, Gaithersburg, Maryland, 1989).
136. M. Fukushima, *Trans. JAR* **7**(3):243 (1990).
137. L. A. Weber and J. M. H. Levelt Sengers, *Fluid Phase Equil.* **55**:241 (1990).
138. M. Fukushima, *Trans. JAR* **8**(1):65 (1991).
139. C. Yokoyama and S. Takahashi, *Fluid Phase Equil.* **67**:227 (1991).
140. H. Sunaga, R. Tillner-Roth, H. Sato, and K. Watanabe, *Int. J. Thermophys.* **19**:1623 (1998).
141. D. R. Defibaugh and G. Morrison, *Fluid Phase Equil.* **80**:157 (1992).
142. S. J. Boyes and L. A. Weber, *J. Chem. Thermodyn.* **27**:163 (1995).
143. F. Ye, H. Sato, and K. Watanabe, *J. Chem. Eng. Data* **40**:148 (1995).
144. H. A. Duarte-Garza, C. E. Stouffer, K. R. Hall, J. C. Holstee, K. N. Marsh, and B. E. Gammon, *J. Chem. Eng. Data* **42**:745 (1997).
145. K. Kraft and A. Leipertz, *Int. J. Thermophys.* **15**:387 (1994).
146. T. Hozumi, H. Sato, and K. Watanabe, *Int. J. Thermophys.* **17**:587 (1996).
147. K. A. Gillis, *Int. J. Thermophys.* **18**:73 (1997).
148. C. M. Bignell and P. J. Dunlop, *J. Chem. Phys.* **98**:4889 (1993).
149. Y. Monluc, T. Sagawa, H. Sato, and K. Watanabe, Thermodynamic Properties of HFC-125, in *Proc. 12th Japan Symp. Thermophys. Prop.* (1995).
150. L. C. Wilson, W. V. Wilding, G. M. Wilson, R. L. Rowley, V. M. Felix, and T. Chilsom-Carter, *Fluid Phase Equil.* **80**:167 (1992).

151. T. Sagawa, *Thermodynamic Properties of HFC-125 by a Constant-Volume Method* (M.S. Thesis, Keio University, Yokohama, 1994).
152. T. Sagawa, H. Sato, and K. Watanabe, *High Temp.–High Press.* **26**:193 (1994).
153. Y. Higashi, *Int. J. Refrig.* **17**:524 (1994).
154. S. Kuwabara, H. Aoyama, H. Sato, and K. Watanabe, *J. Chem. Eng. Data* **40**:112 (1995).
155. L. A. Weber, *Int. J. Thermophys.* **10**:617 (1989).
156. C. C. Piao, H. Sato, and K. Watanabe, *ASHRAE Trans.* **96**:132 (1990).
157. S. Tang, G. X. Jin, and J. V. Sengers, *Int. J. Thermophys.* **12**:515 (1991).
158. H. Hou, J. C. Holste, B. E. Gammon, and K. N. Marsh, *Int. J. Refrig.* **15**:365 (1992).
159. J. W. Magee, *Int. J. Refrig.* **15**:372 (1992).
160. Z. Y. Quian, H. Sato, and K. Watanabe, *Fluid Phase Equil.* **78**:323 (1993).
161. R. Tillner-Roth and H. D. Baehr, *J. Chem. Thermodyn.* **24**:413 (1992).
162. M. Dressner and K. Bier, *Thermische Mischungseffekte in binären Gasmischungen mit neuen Kältemitteln.* Fortschr.-Ber. VDI, Reihe 3, 332 (1993).
163. J. Klomfar, J. Hruby, and O. Sifner, *Int. J. Thermophys.* **14**:727 (1993).
164. R. Tillner-Roth and H. D. Baehr, *J. Chem. Thermodyn.* **25**:277 (1993).
165. A. R. H. Goodwin and M. R. Moldover, *J. Chem. Phys.* **93**:2741 (1990).
166. T. Takagi, *JAR and Japan Flon Gas Assoc.* 56 (1991).
167. H. J. R. Guedes and J. A. Zollweg, *Int. J. Refrig.* **15**:381 (1992).
168. W. Beckermann, *Messung der Schallgeschwindigkeit an Arbeitsstoffen der Energietechnik.* Fortschr.-Ber. VDI, Reihe 19, 67 (1993).
169. A. Saitoh, S. Nakagawa, H. Sato, and K. Watanabe, *J. Chem. Eng. Data* **35**:107 (1990).
170. S. Nakagawa, H. Sato, and K. Watanabe, Specific heat at constant pressure for liquid new refrigerants, in *Proc. 27th Nat. Heat Trans. Symp. Japan,* (Nagoya, 1990).
171. G. Ernst, G. Bräuning, J. Gürtner, Y. J. Parks, and H. Wirbser, Experimental results for R-134a, Private communication (Universität Karlsruhe, 1992).
172. H. Wirbser, *Hochdruckströmungskalorimetrie: Spezifische Wärmekapazitäten und differentieller Joule-Thomson-Koeffizient halogenisierter Kohlenwasser-stoffe* (Ph.D. thesis, Universität Karlsruhe, 1994).
173. W. Blanke, G. Klingenberg, and F. Weber, *Int. J. Thermophys.* **19**:653 (1998).
174. H. D. Baehr and R. Tillner-Roth, *J. Chem. Thermodyn.* **23**:1063 (1991).
175. J. W. Magee and J. B. Howley, *Int. J. Refrig.* **15**:362 (1992).
176. A. R. H. Goodwin, D. R. Defibaugh, and L. A. Weber, *Int. J. Thermophys.* **13**:837 (1993).
177. E. W. Lemmon and R. T Jacobsen, *J. Phys. Chem Ref. Data* **29**:521 (2000).
178. G. Giuliani, S. Kumar, F. Polonara, and D. Zazzini, Experimental determination of vapour pressure of 1,1,1-trifluoroethane (R-143a), in *Proc. of the Joint Meeting of IIR Com. B1, B2, E1, and E2* (Padova, Italy, 1994).
179. G. Giuliani, S. Kumar, F. Polonara, and D. Zazzini, *J. Chem. Eng. Data* **40**:903 (1995).
180. H.-L. Zhang, H. Sato, and K. Watanabe, *J. Chem. Eng. Data* **40**:887 (1995).
181. L. A. Weber and D. R. Defibaugh, *J. Chem. Eng. Data* **41**:1477 (1996).
182. D. R. Defibaugh and M. R. Moldover, *J. Chem. Eng. Data* **42**:160 (1997).
183. J. W. Magee, *Int. J. Thermophys.* **19**:1381 (1998).
184. J. W. Magee, *Int. J. Thermophys.* **19**:1397 (1998).
185. W. Beckermann and F. Kohler, *Int. J. Thermophys.* **16**:445 (1995).
186. H. Russel, D. R. V. Golding, and D. M. Yost, *J. Am. Chem. Soc.* **66**:16 (1944).
187. S. L. Outcalt and M. O. McLinden, *J. Phys. Chem. Ref. Data* **25**:605 (1996).
188. V. Z. Geller, E. G. Porichanski, P. I. Svetlichnyi, and Y. G. Elkin, *Kholod. Tekh.* **29**:43 (1980).

189. W. Blanke and R. Weiß, *Fluid Phase Equil.* **80**:179 (1992).
190. T. Hozumi, T. Koga, H. Sato, and K. Watanabe, *Int. J. Thermophys.* **14**:739 (1993).
191. K. Kraft and A. Leipertz, *Int. J. Thermophys.* **15**:791 (1994).
192. E. G. Porichanski, O. P. Ponomareva, and P. I. Svetlichny, *Izv. Vyssh. Uchebn. Zaved Energ.* **3**:122 (1982).
193. W. Benade, *Bestimmung der thermophysikalischen Eigenschaften alternativer Kältemittel* (Ph.D. thesis, University Essen, 1993).
194. S. Nakagawa, T. Hori, H. Sato, and K. Watanabe, *J. Chem. Eng. Data* **38**:70 (1993).
195. A. Iso and M. Uematsu, *Phys. A* **156**:454 (1989).
196. T. Tamatsu, T. Sato, H. Sato, and K. Watanabe, *Int. J. Thermophys.* **13**:985 (1992).
197. M. Türk, J. Zhai, M. Nagel, and K. Bier, *Messung des Dampfdruckes und der kritischen Zustandsgrößen von neuen Kältemitteln.* Fortschr.-Ber. VDI, Reihe 19, 79 (1994).
198. H. Sato, M. Uematsu, and K. Watanabe, *Fluid Phase Equil.* **36**:167 (1987).
199. A. Valtz, S. Laugier, and D. Richon, *J. Chem. Eng. Data* **32**:397 (1987).
200. A. Michels, C. Michels, and H. Wouters, *Proc. Roy. Soc. A* **153**:214 (1935).
201. M. P. Vukalovich and V. V. Altunin, *Teploenergetica* **9**(5):56 (1962).
202. J. Juza, V. Kmonicek, and O. Sifner, *Physica* **31**:1735 (1965).
203. V. A. Kirillin, S. A. Ulybin, and E. P. Zherdev, *Teploenergetica* **16**(6):92 (1969).
204. V. A. Kirillin, S. A. Ulybin, and E. P. Zherdev, *Teploenergetica* **16**(2):94 (1969).
205. V. A. Kirillin, S. A. Ulybin, and E. P. Zherdev, Experimental investigation of carbon dioxide density at temperatures from −50 to +200°C and pressures up to 500 bar, in *Proc. 1st Intern. Conf. Calorimetry and Thermodynamics,* (Warsaw, 1969).
206. V. A. Kirillin, S. A. Ulybin, and E. P. Zherdev, *Teploenergetica* **17**(5):69 (1970).
207. V. N. Popov and M. K. Sayapov, *Teploenergetica* **17**(4):76 (1970).
208. W.-W. R. Lau, *A Continuously Weighed Pycnometer Providing Densities for Carbon Dioxide+Ethane Mixtures Between 240 and 350 K at Pressures up to 35 MPa* (Ph.D. thesis, Texas A&M University, 1986).
209. G. J. Esper, *Direkte und Indirekte pvT-Messungen an Fluiden,* (Ph.D. thesis, Ruhr-Universität Bochum, 1987).
210. J. C. Holste, K. R. Hall, P. T. Eubank, G. Esper, M. Q. Warowny, D. M. Bailey, J. G. Young, and M. T. Bellamy, *J. Chem. Thermodyn.* **19**:1233 (1987).
211. M. Jaeschke, *pρT Data from Refractive-index Measurements,* Private communication, (Ruhrgas AG, Essen, 1987).
212. M. Jaeschke, *pρT Data from Burnett Measurements,* Private communication (Ruhrgas AG, Essen, 1987).
213. J. W. Magee and J. F. Ely, *Int. J. Thermophys.* **9**:547 (1988).
214. J. F. Ely, W. M. Haynes, and B. C. Bain, *J. Chem. Thermodyn.* **21**:879 (1989).
215. W. Duschek, R. Kleinrahm, and W. Wagner, *J. Chem. Thermodyn.* **22**:827 (1990).
216. M. Jaeschke, A. E. Humphreys, P. Van Caneghem, M. Fauveau, R. Janssen-Van Rosmalen, and Q. Pellei, *GERG Technical Monograph 4–The GERG Databank of High Accuracy Compressibility Factor Measurements,* Edited by the Group Europeen de Recherches Gazieres, (VDI, Düsseldorf, 1990).
217. R. Gilgen, R. Kleinrahm, and W. Wagner, *J. Chem. Thermodyn.* **24**:1493 (1992).
218. X. Y. Guo, R. Kleinrahm, and W. Wagner, *Experimentelle Untersuchung der systematischen Meßfehler von Betriebsdichteaufnehmern für Erdgas-Meßstrecken–Teil 1: Meßergebnisse für Stickstoff, Kohlendioxid, Argon, Neon, Ethan und Ethen,* Report Lehrstuhl für Thermodynamik (Ruhr-Universität Bochum, 1992).
219. K. Brachthäuser, R. Kleinrahm, H.-W. Lösch, and W. Wagner, *Entwicklung eines neuen Dichtemeßverfahrens und Aufbau einer Hochtemperatur-Hochdruck-Dichtemeßanlage,* Fortschr.-Ber. VDI, Reihe 8, 371 (1993).

220. A. Fenghour, W. A. Wakeham, and J. T. R. Watson, *J. Chem. Thermodyn.* **27**:219 (1995).
221. P. Nowak, Th. Tielkes, R. Kleinrahm, and W. Wagner, *J. Chem. Thermodyn.* **29**:885 (1997).
222. J. Klimeck, R. Kleinrahm, and W. Wagner, *J. Chem. Thermodyn.* (in press).
223. J. W. Magee and J. F. Ely, *Int. J. Thermophys.* **7**:1163 (1986).
224. I. M. Abdulagatov, N. G. Polikhronidi, and R. G. Batyrova, *Ber. Bunsenges. Phys. Chem.* **98**:1068 (1994).
225. I. I. Novikov and Y. S. Trelin, *Zur. Prik. Mech. Tech. Fiz.* **2**:112 (1960).
226. I. I. Novikov and Y. S. Trelin, *Teploenergetica* **9**(2):79 (1962).
227. W. Pecceu and W. Van Dael, *Physica* **63**:154 (1972).
228. R. Bender, K. Bier, and G. Maurer, *Ber. Bunsenges. Phys. Chem.* **85**:778 (1981).
229. G. Ernst, G. Maurer, and E. Wiederuh, *J. Chem. Thermodyn.* **21**:53 (1989).
230. G. Ernst and U. E. Hochberg, *J. Chem. Thermodyn.* **21**:407 (1989).
231. D. Möller, B. E. Gammon, K. N. Marsh, K. R. Hall, and J. C. Holste, *J. Chem. Thermodyn.* **25**:1273 (1993).
232. W. Duschek, R. Kleinrahm, and W. Wagner, *J. Chem. Thermodyn.* **22**:841 (1990).
233. C. H. Meyers and R. S. Jessup, *Refrig. Eng.* **11** (10):345 (1925).
234. J. A. Beattie and Ch. K. Lawrence, *J. Am. Chem. Soc.* **52**:6 (1930).
235. A. Kumagi and T. Toriumi, *J. Chem. Eng. Data* **16**:293 (1971).
236. K. Date, *Rev. Phys. Chem. Japan* **43**:1 (1973).
237. H. Garnjost, *Druck–Volumen–Temperaturmessungen mit Ammoniak und Wasser*. (Ph.D. thesis, Ruhr-Universität Bochum, 1974).
238. M. Zander and W. Thomas, *J. Chem. Eng. Data* **24**:1 (1979).
239. M. H. Streatfield and C. Henderson, *J. Chem. Thermodyn.* **19**:1163 (1987).
240. S. Glowka, *Pol. J. Chem.* **64**:699 (1990).
241. F. Harms-Watzenberg, *Messung und Korrelation der thermodynamischen Eigenschaften von Wasser-Ammoniak Gemischen*. Fortschr.-Ber. VDI, Reihe 3, 380 (1995).
242. Yu. P. Blagoi, A. E. Butko, S. A. Mikhailenko, and V. V. Yakuba, *Russian J. Phys. Chem.* **42**:564 (1968).
243. N. S. Osborne and M. S. van Dusen, *Bur. of Stand. Bull.* **14**:397 (1918).
244. N. S. Osborne, H. F. Stimson, T. S. Sligh, and C. S. Cragoe, *Sci. Pap. Bur. Stand.* **20**:65 (1925).
245. R. Overstreet and W. F. Giauque, *J. Am. Chem. Soc.* **59**:254 (1937).
246. C. S. Cragoe, C. H. Meyers, and C. S. Taylor, *Sci. Pap. Bur. Stand.* **16**:1 (1920).
247. A. Stock, F. Henning, and E. Kuss, *Ber. Dtsch. Chem. Ges.* **54**:1119 (1921).
248. C. S. Cragoe and D. R. Harper, *ASRE J.* **7** (2):113 (1920).
249. W. S. Groenier and G. Thodos, *J. Chem. Eng. Data* **5**:285 (1960).
250. C. S. Cragoe, E. C. McKelvy, and G. F. O'Connor, *Sci. Pap. Bur. Stand.* **18**:707 (1922).
251. G. Herres and D. Gorenflo, *First Attempts to Describe Associating Fluids by Adding Physically Motivated Terms to an Empirical Equation of State,* Private communication (Universität Paderborn, 2000).